The impacts of intensive mining on terrestrial and aquatic ecosystems: a case of sediment pollution and calcium decline in cool temperate Tasmania, Australia

Beck, K.K.[1,2*], Mariani, M.[2,3,4], Fletcher, M-S.[2], Schneider, L.[4], Aquino-López, M. A.[5], Gadd, P.S.[6], Heijnis, H.[6], Saunders, K.M. [6] & Zawadzki, A.[6]

[1]Lincoln Centre for Water and Planetary Health, School of Geography, University of Lincoln, Lincoln, UK

[2]School of Geography, University of Melbourne, Melbourne, Australia

[3]School of Geography, University of Nottingham, Nottingham, UK

[4]ANU College of Asia and the Pacific, Australian National University, Canberra, Australia

[5]Maynooth University, Arts and Humanities Institute, Maynooth, Co. Kildare, Ireland.

[6]Australian Nuclear Science and Technology Organisation, Lucas Heights, Australia

**corresponding author kbeck@lincoln.ac.uk*

Keywords:

diatoms; mining; heavy metals; sediment pollution; Ca decline; Tasmania

Graphical Abstract

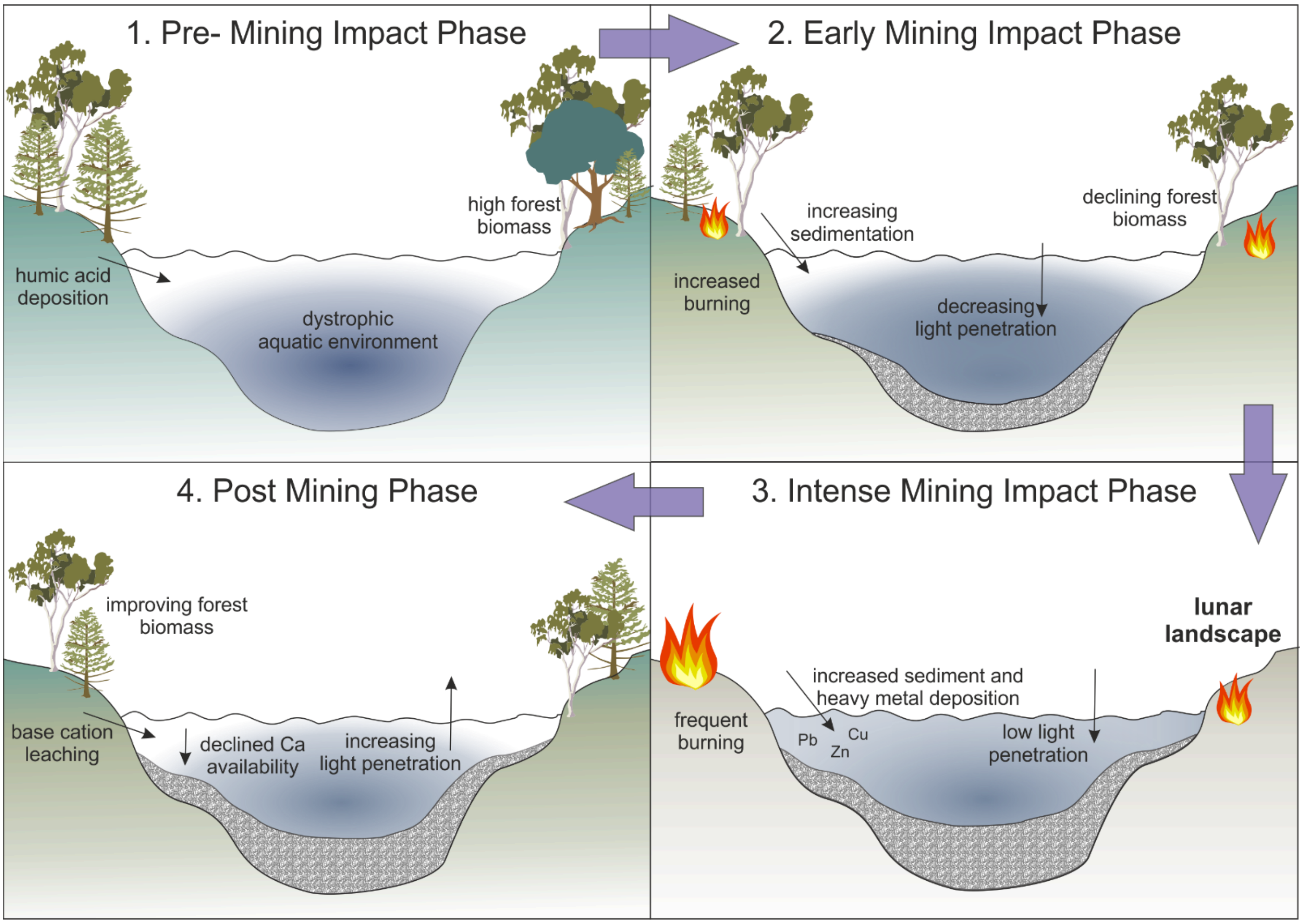

Abstract:

Mining causes extensive damage to aquatic ecosystems via acidification, heavy metal pollution, sediment loading, and Ca decline. Yet little is known about the effects of mining on freshwater systems in the Southern Hemisphere. A case in point is the region of western Tasmania, Australia, an area extensively mined in the 19th century, resulting in severe environmental contamination. In order to assess the impacts of mining on aquatic ecosystems in this region, we present a multiproxy investigation of the lacustrine sediments from Owen Tarn, Tasmania. This study includes a combination of radiometric dating (^{14}C and ^{210}Pb), sediment geochemistry (XRF and ICP-MS), pollen, charcoal and diatoms. Generalised additive mixed models were used to test if changes in the aquatic ecosystem can be explained by other covariates. Results from this record found four key impact phases: (1) Pre-mining, (2) Early mining, (3) Intense mining, and (4) Post-mining. Before mining, low heavy metal concentrations, slow sedimentation, low fire activity,

and high biomass indicate pre-impact conditions. The aquatic environment at this time was oligotrophic and dystrophic with sufficient light availability, typical of western Tasmanian lakes during the Holocene. Prosperous mining resulted in increased burning, a decrease in landscape biomass and an increase in sedimentation resulting in decreased light availability of the aquatic environment. Extensive mining at Mount Lyell in the 1930s resulted in peak heavy metal pollutants (Pb, Cu and Co) and a further increase in inorganic inputs resulted in a disturbed low light lake environment (dominated by *Hantzschia amphioxys* and *Pinnularia divergentissima*). Following the closure of the Mount Lyell Co. in 1994 CE, Ca declined to below pre- mining levels resulting in a new diatom assemblage and deformed diatom valves. Therefore, the Owen Tarn record demonstrates severe sediment pollution and continued impacts of mining long after mining has stopped at Mt. Lyell Mining Co.

Capsule of main findings

The Owen Tarn record revealed four impact phases: Pre- mining, Early mining, Intense mining, and Post mining. Mining caused severe sediment pollution and Ca decline in the aquatic environment.

1.1 Introduction

The industrial revolution initiated significant land-use change resulting in extensive environmental degradation across the globe. Amongst this environmental damage, aquatic ecosystems were gravely impacted by eutrophication, deforestation, climate change, pollution, and acidification (Mills et al., 2017). Mining in particular has been a major cause of freshwater disturbance; where heavy metal pollution, acidification, sediment loading, de-oxygenation, salinization, and calcium (Ca) declines have had negative consequences on aquatic ecosystem health (Augustinus et al., 2010; Battarbee, 1984; Hodgson et al., 2000; Jeziorski et al., 2008; Schneider et al., 2019; Sienkiewicz and Gąsiorowski, 2016; Teasdale et al., 2003; Younger and Wolkersdorfer, 2004). Due to the importance of freshwater to all life on Earth, it is crucial to understand the impacts of mining on these systems. Recent work on heavy metal pollution in Tasmania, Australia has found that this island has some of the most severely contaminated sediments worldwide (Schneider et al., 2019), yet, there is limited understanding of how aquatic environments have been impacted. Here we explore the palaeoenvironmental history of a lake near Queenstown, Tasmania to assess the impacts of mining on the aquatic environment.

The geological activity in Tasmania has resulted in abundant ore deposits that were extracted in the 19th and 20th centuries for gold, copper, lead, zinc, tin and silver (McQuade et al., 1995). One such region, Queenstown, was mined extensively from the late 1800's (Corbett, 2001) and has been a focus area to study the impacts of mining on the environment (Augustinus et al., 2010; Harle et al., 2002; Hodgson et al., 2000; McMinn et al., 2003; Schneider et al., 2019). Mining in this region has caused extensive heavy metal pollution and mass deforestation from clearance, smelting, and acid deposition leading to high sediment loading and contamination in waterways (Augustinus et al., 2010; Knighton, 1989; Norris and Lake, 1984; Saunders et al., 2013; Schneider et al., 2019; Seen et al., 2004). An estimated 95 Mt of tailings discharge and 1.4 Mt of smelting slag was deposited into nearby river systems (Augustinus et al., 2010) causing metal contamination and acidified waterways of the King-Henty catchment (Augustinus et al., 2010; Teasdale et al., 2003). Additionally, it has been suggested, by a palaeolimnological study, that a nearby lake has been impacted by acidification from local mining and sulphate deposition. With the closing of the Mount (Mt.) Lyell Mine Co. in 1994 CE, this lake has shown evidence of acidification recovery (Hodgson et al., 2000). However, the lack of chronology in this palaeolimnological record leaves the question of pre-impact conditions and whether the aquatic environment is reflecting changing acidity. Due to the severity of contamination in this region, it is imperative to understand the ecological impacts and baseline conditions of these systems if we are to restore them to pre-impact environments.

Environmental recovery of aquatic systems (both chemical and/or biological) post mining is possible (Findlay, 2003; Graham et al., 2007; Keller et al., 1992; Keller et al., 1998); however, many lakes still have not achieved full biological recovery (Battarbee et al., 1988; Sienkiewicz and Gąsiorowski, 2016; Stoddard et al., 1999). In some circumstances, this is due to multiple environmental stressors impacting the biological communities (i.e. climate change) (Arseneau et al., 2011) or secondary impacts of mining (i.e. Ca decline or phosphorus availability) (Jeziorski et al., 2008; Kopáček et al., 2015). Reductions in Ca content of freshwater is an emerging issue from industrial acidifying emissions. For example, soft water lakes in Canada have experienced Ca declines due to past mining, irrespective of pH recovery (Barrow et al., 2014; Jeziorski et al., 2008). Acidic sulphur oxide emissions from mining resulted in leaching of available soil base cations to buffer watersheds from acid deposition. While emissions are on the decline, base cations are still experiencing long-term declines from delayed recovery of replenished stocks (Barrow et al., 2014; Graham et al., 2007; Jeziorski et al., 2008). Tasmania has had a similar history of mining to North America and there are suggestions of lake acidification caused by mining (Hodgson et al., 2000); however, the secondary impacts of mining, such as Ca decline, have not been explored.

Here we re-investigate the palaeoenvironmental history of Owen Tarn, Tasmania, a site that shows the highest levels of heavy metal contamination in the region (Schneider et al., 2019), to understand the impacts of mining on aquatic ecosystems and determine if the environment has recovered to baseline conditions. We aim to address the following questions: 1) What are the aquatic ecosystem baseline conditions at Owen Tarn?, 2) Was the aquatic and terrestrial environment impacted by mining? If so how?, and 3) Has the aquatic biota and local vegetation recovered to pre-disturbance conditions since the Mt. Lyell mine closed? Using a multiproxy palaeoenvironmental approach we constructed a chronology of pre- and post-mining impact using radiometric dating (radiocarbon and lead-210). Sediment geochemistry (X-Ray Fluorescence and Inductively coupled plasma mass spectrometry) was used to determine the extent of mining and heavy metal pollution within the lake along with pollen, charcoal and diatoms to assess the aquatic and terrestrial ecosystem response and potential recovery from mining impacts.

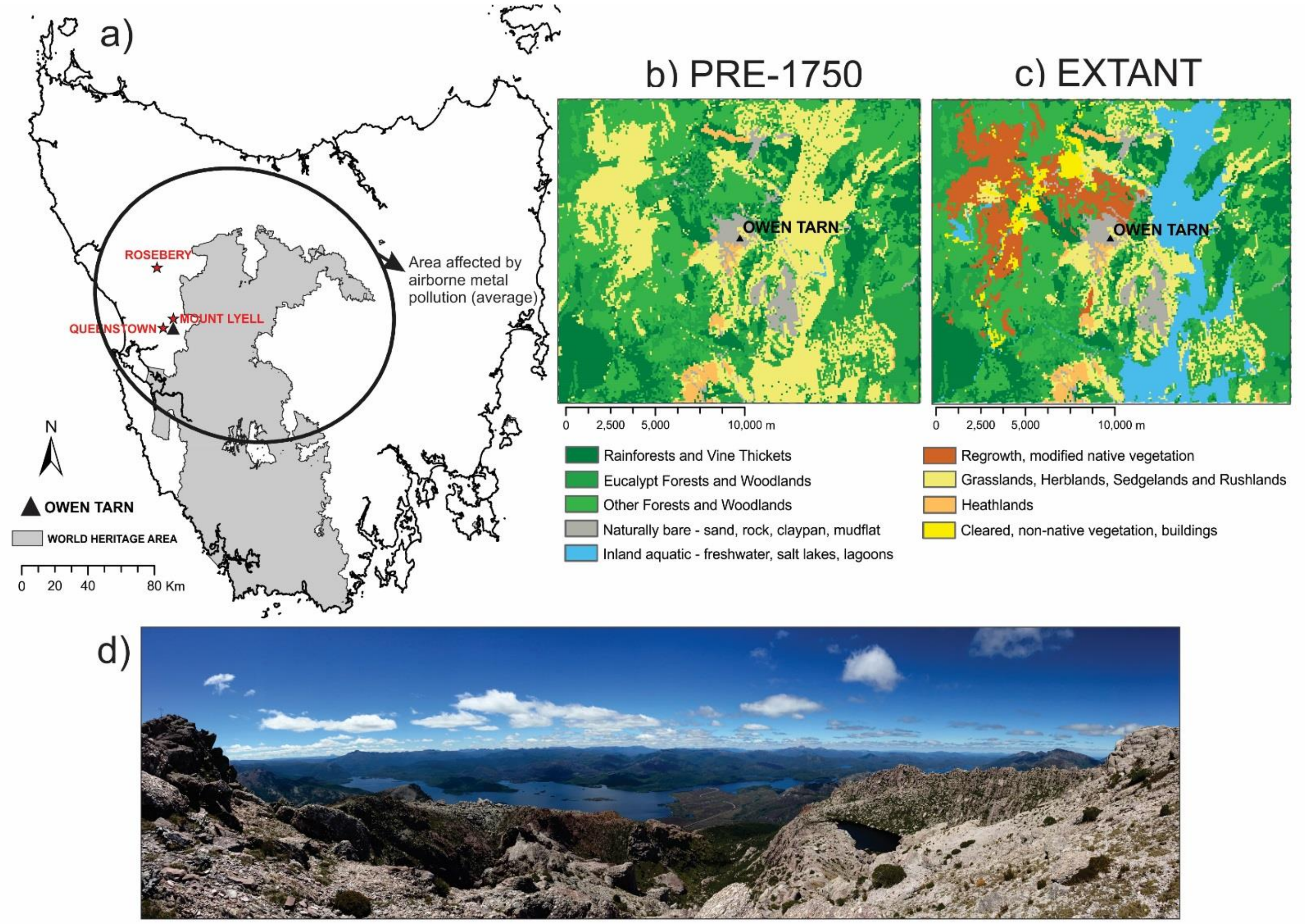

Figure 1: a) Map of Tasmania with a black ellipsis indicating the projected metal deposition from 1961–1990 CE (Schneider et al., 2019) and locations of Owen Tarn (black triangle), Rosebery, Queenstown, and Mount Lyell (red stars). Major vegetation groups surrounding Owen Tarn b) pre 1750 CE (National Vegetation Information System, 2018a) and c) extant vegetation groups (National Vegetation Information System, 2018b). d) Photograph of Owen Tarn taken by Dr. Michael-Shawn Fletcher (2015).

1.2 Mining History of Queenstown

Mt. Lyell, located ~6 km from Queenstown, Tasmania, was one of Australia's oldest and most successful mines due to high sulphur content and abundance of timber for fuel (Keele, 2003). British exploration of Tasmania began in the early 1800s (Harle et al., 2002) and by 1850 CE western Tasmanian geological deposits were being explored during the excitement of the gold-rush (Bottrill, 2000; Keele, 2003). In 1892 CE the Mt. Lyell Mining company began with the discovery of high copper ore samples and thus began smelting for copper, tin, silver, gold, lead and zinc (McQuade et al., 1995). The start of commercial mining created settlement and the establishment of rails and infrastructure in mining towns such as Queenstown, Rosebery, Gormanston, Linda, and Crotty, Tasmania. The Mt. Lyell Mining Co. peaked in efficiency with maximum ore production from the 1930s to 80s when the West Lyell open-cut site was in operation, producing 500,000-2,000,000 tons of tailings per year (McQuade et al., 1995). Smelting ceased at Mount Lyell by 1969 CE when ore was shipped to other regions in Tasmania, and by the 1980s mining across Tasmania was on the decline (McQuade et al., 1995). The Mt. Lyell Mining Co. finally closed down in 1994 CE (Teasdale et al., 2003). Environmental degradation of this region was so extensive that much of the lush temperate rainforests and sclerophyll forests turned into a 'lunar landscape' (Bowman et al., 2011; Keele, 2003) with severe heavy metal contamination remaining in the landscape today (Schneider et al., 2019).

2. Methods

2.1 Study Site

Owen Tarn (42°05'58" S, 145°36'33" E) is a small cirque lake (lake area <0.013 km^2), 1,210 meters above sea level located ~5 km southeast of the Mt. Lyell mine (Figure 1). The lake is located in the upper catchment receiving no inflowing water from other lakes or rivers. Owen Tarn sits in the western limnological province of Tasmania where lakes are acidic, dystrophic and oligotrophic (Buckney and Tyler, 1973; Tyler, 1974, 1992; Vyverman et al., 1995). The total annual rainfall at Owen Tarn is ~2800 mm with an average annual temperature of ~8.6 °C (Mariani et al., 2019; Schneider et al., 2019). Currently, the catchment is mostly exposed bedrock with sparse western subalpine scrub including species *Agatachys odorata, Cenarrhenes nitida, Eucalyptus vernicosa*, *Leptospermum nitridium,* and *Monotoca submutica* (Hodgson et al., 2000; Mariani et al., 2019). Geology around Owen Tarn is described as poorly buffering upper Cambrian- lower Ordovician Owen Conglomerate (Hodgson et al., 2000).

2.2 Coring and Chronology

In 2015 Owen Tarn was sampled using a Universal corer at a maximum depth of 7 m. A 69 cm surface core (TAS1501) was extracted but only the top 25 cm were analysed in this study.

To construct a reliable chronology a Bayesian age-depth model was created in *Plum* (Aquino-López et.al 2018). *Plum* is a new approach to ^{210}Pb dating constructed under a Bayesian framework that uses raw ^{210}Pb concentrations to construct an age-depth model as well as its uncertainties. This approach calculates the chronology using the total ^{210}Pb concentration and infers the supported ^{210}Pb as one of the parameters of the model; this reduces the input of the researcher. One of the benefits of *plum* is the ability to naturally incorporate ^{210}Pb data into chronologies where other isotopes are also measured, such as radiocarbon. It is important to mention that this approach does not require the pre-modelling of ^{210}Pb as is common practice when merging ^{210}Pb into longer chronologies with radiocarbon. The age-depth model was created with the *plum* package *v. 0.1.0* (Aquino-López, 2018) in *R (the package can be obtained from https://github.com/maquinolopez)*.

In the top 25 cm, eight ^{210}Pb dates were analysed using alpha spectrometry and two radiocarbon samples were analysed at Australian Nuclear Science and Technology Organisation (ANSTO) to create a chronology for the sediment sequence. The bottom two ^{210}Pb samples had reached background conditions (Table 1: samples S391 and S392). Due to the limited number of ^{210}Pb samples for the age-depth model, the heavy metal profile of Zinc (Zn) was used as a chronological marker for mining activity. Zn was chosen as the chronological marker because (a) it was mined in Queenstown, Tasmania (McQuade et al., 1995), (b) it has a depositional profile consistent with mining activity in this area (Fig. 2), and (c) Zn shows little to no post-depositional mobility (Andrade et al., 2010; Augustinus et al., 2010; Kaasalainen and Yli-Halla, 2003; Schneider et al., 2019). The date 1885 CE ± 2.5 was assigned to the age-model as an additional age horizon with the initial rise in Zn (between 18 and 19 cm) with the start of commercial mining in the 1880s (yellow circles, Fig. 2f).

A radiocarbon reservoir was calculated to correct bulk sediment samples for remobilisation of ‘old’ carbon on the landscape into depositional environments which produce anomalously old radiocarbon ages (Bertrand et al., 2012). To calculate the reservoir effect, an offset variable was added to the radiocarbon dates of the age-depth model using the offset between the ^{210}Pb and ^{14}C data and estimated as part of the Marko Chain Monte Carlo process in *Plum* (see Fig. 2e). This approach allowed uncertainties related to the reservoir effect to be calculated by the *Plum* model and incorporated into chronology.

2.3 Geochemistry

X-ray fluorescence (XRF) and inductively coupled plasma mass spectrometry (ICP-MS) were used to retrieve geochemical trends in the sedimentary record. XRF analysis was performed using an Itrax micro X-ray fluorescence core scanner at ANSTO at 0.1 cm intervals with a dwell time of 10s using a molybdenum (Mo) tube set to 30kV and 55mA. Select elements from the XRF results were used in this study: Pb, Br, Si, Ti, and Inc/coh (more elemental data can be found in the Supplementary Data). Molybdenum Incoherent/coherent ratio (Inc/coh) approximates the average matrix composition of atomic numbers and was used to estimate organic matter content in sediment archives (Croudace and Rothwell, 2015; Field et al., 2018; Woodward and Gadd, 2019; Woodward et al., 2018). Br was used as another indicator for organic rich sediments (Croudace and Rothwell, 2015; Fedotov et al., 2015; Ziegler et al., 2008).

ICP-MS analysis was performed at 1 cm intervals. Sediment samples were freeze-dried for 72 h and placed into 200 mL tubes where they were homogenized by intensive manual mixing of sediment. Approximately 0.2 g of freeze-dried material was weighed into a 60 mL polytetrafluoroacetate (PFA) closed digestion vessel (Mars Express) and 2 mL of concentrated nitric acid (Aristar, BDH), and 1 mL of 30% concentrated hydrochloric acid (Merck Suprapur, Germany) was added (Telford et al., 2008). Each PFA vessel was then capped, placed into a 800 W microwave oven (CEM model MDS-81, Indian Trail, NC, USA) and heated at 120ºC for 15 min. The samples were cooled to room temperature and diluted with 50 mL of deionised water (Sartorius, Australia). Then centrifuged at 5000 rpm for 10 min and 1 mL of the digest was transferred into a 10-mL centrifuge tube and diluted to 10 mL with ICP-MS internal standard (Li^{6}, Y^{19}, Se^{45}, Rh^{103}, In^{116}, Tb^{159} and Ho^{165}). Digests were stored (at 5ºC) until analysed using an inductively coupled plasma mass spectrometer (PerkinElmer DRC-e) with an AS-90 autosampler (Maher et al., 2001). The certified reference NIST- 2710 (Montana Soil I) and NWRI WQB-1 (Lake Ontario sediment) were used as controls to check the quality and traceability of metals, and whether measured concentrations were in at least 90% agreement with certified values.

2.4 Charcoal and Pollen

Macroscopic charcoal was processed at 0.5 cm intervals by standard protocol (Whitlock and Larsen, 2001) using 1.25 ml of sample in household bleach for a week. The charcoal accumulation rate (CHARacc) was calculated using the sum of the macroscopic charcoal particles divided by the sample volume and sediment accumulation rate. Pollen samples were processed at 0.5 cm intervals using 0.5 ml of sediment by standard protocols (Faegri and Iversen, 1989). A minimum of 300 terrestrial pollen grains were identified in each sample. Percentages were calculated using the sum of terrestrial pollen. Other aquatic pollen and spores percentages were calculated using the sum of the terrestrial pollen in addition to the sum of aquatic pollen and spores. Stratigraphically constrained cluster analysis (CONISS) (Grimm, 1987) was used to produce a dendrogram for the terrestrial pollen data and a broken stick model determined the number of significant zones using the package *rioja v. 0.9-15.1* (Juggins, 2018) in *R*. A principal component analysis (PCA) was performed on all terrestrial pollen grains using the *vegan* package *v. 2.5-4* (Oksanen et al., 2019) in *R* with a standardized transformation method which scales data to a mean of zero and units of variance.

2.5 Diatoms

Diatoms were processed at 0.5 cm intervals from 0 to 2 cm and 1 cm intervals from 2 to 24 cm using standard protocols (Battarbee, 1986). A minimum of 300 diatom valves were identified per slide; however, due to low concentrations of some sample depths (0.5, 1.0, 1.5, 2.0, 3.0, 5.0, 9.0, and 11.0 cm), a minimum of 100 valves were identified. Valve concentration was estimated using the known volume of sediment via the evaporation method (Battarbee, 1986) and mounted using Naphrax®. Species were identified using an oil immersion DIC objective at 1000x magnification and taxonomic nomenclature was verified using Algaebase (http://www.algaebase.org/) (see Supplementary data Table S3 for authority names). The relative species abundances were calculated using the sum of all species. CONISS was applied to the entire diatom dataset to create a dendrogram and a broken stick model was used to determine the number of significant zones with *rioja.* A PCA was performed on diatom percent abundance that occurred at least three times with an abundance greater than 2% using the standardize method in *vegan.*

2.6 Generalised additive mixed models

Generalised additive mixed models (GAMMs) can be used to test if changes in a curve are a function of other predictors. The GAMMs were used to test if shifts in diatom response (i.e. PCA 1) could be explained by other covariates (or proxies) of the time series data. GAMMs use random effects nonparametric statistics and the sum of smooth functions to model the explanatory variables embedded with mixed effect models (fixed and random effects). Fixed effects are used on the explanatory variable and wigglyness from the smooth components uses random effects treatment (Simpson and Anderson, 2009; Sóskuthy, 2017; Wood, 2016). For more comprehensive details of GAMM modelling see Simpson and Anderson (2009). The models were run in *R* using the mgcv package *v. 1.8-28* (Wood, 2016) with the residual maximum likelihood (REML) method to penalise for overfitting trends (Wood, 2016; Wood, 2011), an identity link, and a Gaussian family. GAMMs were individually fitted to diatom PCA axis 1 and axis 2 against binned XRF data (Inc/Coh, Ti and Br) and ICP-MS data (Pb, Ca, and Cu). GAMMs require the covariates and response variables to have the same sample depths. Therefore, XRF data were binned to match diatom sample depths, and diatom samples 0.5 cm and 1.5 cm were excluded when using ICP-MS covariates to match sample depths between proxy datasets (i.e. sample resolution of 1 cm between proxy datasets).

3. Results

3.1 Coring and Chronology

The original core retrieved (TAS1501) from Owen Tarn is 69 cm in length and spans 7,535 yrs (Mariani et al., 2019). However, the record used here focuses on the upper 25 cm spanning ca. 295 yrs due to poor diatom preservation below 25 cm. For detailed core description, see Supplementary data and Figure S1. Table 1 summarises the ^{210}Pb results and Table S1 summarises radiocarbon results spanning the uppermost 25 cm of the sediment core. The unsupported ^{210}Pb activities from this core was relatively low in the upper core depths due to high inorganic content (inorganic fractions peaked at 66.2% with peak mining i.e. 12-14 cm). Some inorganic components remained even after removal of the >63µm fraction. The overall unsupported ^{210}Pb profile exhibits a decreasing trend with depth (See Supplementary Data Fig. S3). The age-depth model was created using *Plum* (Aquino-López et al., 2018) and showed good fit to the ^{210}Pb and ^{14}C results (Fig. 2f) after adjusting for a reservoir effect. The reservoir was so great in Owen Tarn that only the lower end of the probability distributions of the radiocarbon dates appear in Figure 2f. The change in sedimentation is consistent with changes in the deposition processes characterised by the impacts of mining. Upper sediments (0-19 cm) are fast accumulating followed by a shift to slow accumulation from 19-25 cm (Fig. 2). This shift is related to prosperous mining in Queenstown, Tasmania since the 1880s causing increased deposition and the change in sedimentation.

Table 1: Lead-210 results, plum ages, and Constant Rate of Supply (CRS) model.

ANSTO ID	**Core Code**	**Depth (cm)**	**Dry Bulk Density (g/cm^3)**	**Cumulative Dry Mass (g/cm^2) + error**	**Total ^{210}Pb (Bq/kg) + error**	**Plum mean age (yr)**	**Unsupported ^{210}Pb Decay (Bq/kg) + error**	**Calculated CRS age (yrs) + error**
S385	TAS1501	0-0.5	0.63	0.1 ± 0.1	59.1 ± 2.5	0 - 4.58	53.4 ± 2.5	2 ± 2
S386	TAS1501	1-1.5	1.01	1.0 ± 0.2	16.1 ± 0.8	9.166-11.48	12.9 ± 0.8	9 ± 3
S387	TAS1501	3.5-4	1.02	3.5 ± 0.2	8.4 ±0.5	21.32-22.57	4.8 ± 0.6	17 ± 4
S388	TAS1501	5-5.5	0.96	5.0 ± 0.2	11.9 ± 0.7	27.09-29.66	8.7 ± 0.8	22 ± 5
S389	TAS1501	11.5-12	0.74	10.5 ± 0.2	9.5 ± 0.7	66.66-72.42	7.5 ± 0.7	60 ± 8
S390	TAS1501	14-14.5	0.60	12.2± 0.2	8.0 ± 0.7	87.85-92-85	4.5 ± 0.9	82 ± 9
S391	TAS1501	20-20.5	0.61	15.8 ± 0.2	7.9 ± 0.8		1.2 ± 1.1	
S392	TAS1501	25.0-25.5	0.67	19.0 ± 0.2	9.3 ± 0.5		3.4 ± 0.8	

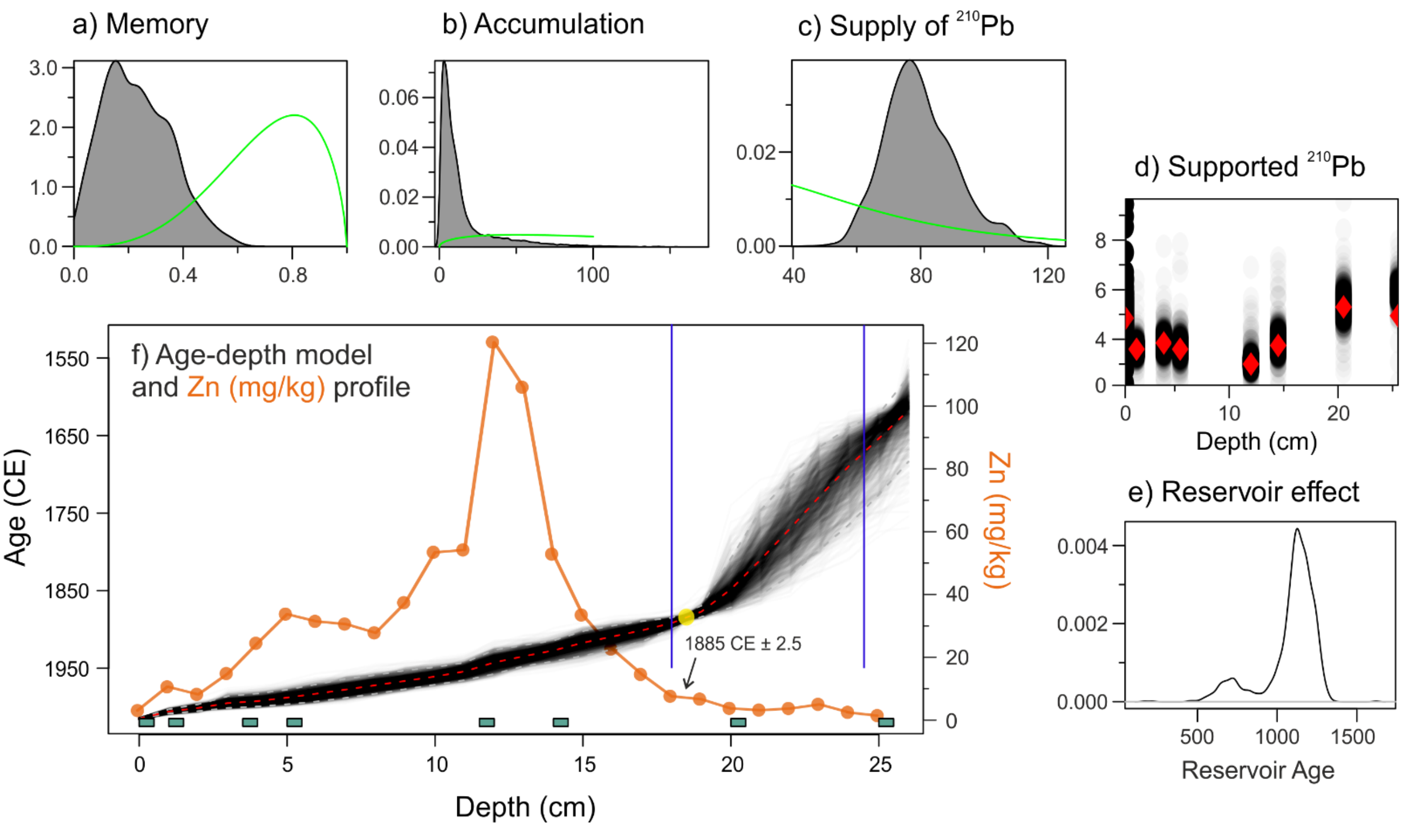

Figure 2: Age depth model results for Owen Tarn top 25cm performed by *Plum* Bayesian statistical modelling (Aquino-López et al., 2018). a) Age model memory, b) accumulation rates, c) supply of ^{210}Pb, d) supported ^{210}Pb by depth (cm), e) reservoir effect, and f) age-depth model (red dashed line) with 95% confidence intervals (grey dashed line) with supported ^{210}Pb samples (green squares) and probability distributions of radiocarbon ages (blue symbols). The yellow circle indicates the mining horizons included in the model (1885 CE ± 2.5 at 18.5 cm) provided by the ICP-MS Zn (mg/kg) profile (orange).

3.2 *Geochemistry*

XRF and ICP-MS results are summarised in Figure 3 with extended results in the Supplementary data (Figs. S1 & S4). Pb_{kcps} is very low at the start of the record and increased rapidly to peak at 12.2 cm (ca. 1941 CE). Br_{kcps} shows low stable values to ~14 cm (ca. 1927 CE) followed by a peak at 12.6 cm (ca. 1938 CE), and gradual decline to present. Ti_{kcps} has a general increasing trend throughout the record. XRF Inc/Coh has a slight increasing trend to maximum values at 13 cm (ca. 1935 CE) followed by a declining trend to minimum values at present. Si_{kcps} shows the opposite trends to Inc/coh with low values from the start of the record followed by an increase at 12.2 cm (ca. 1941 CE) to present. Pb results from the ICP-MS and XRF show consistent trends between the two geochemical analyses (Fig. 3).

ICP-MS Pb, As, Cd, and Se (mg/kg) show similar trends with low values in the early part of the record followed by an increase at ~18 cm (ca. 1892 CE) to peak at 14-12 cm (ca. 1927-1943 CE), followed by a decline to present. Ca (mg/kg) shows the same trends with the exception of a decline beyond background values to a minimum at present. Cu (mg/kg) has low values from 25 to 16 cm (ca. 1654-1909 CE) followed by an incline to peak at 13 cm (ca. 1935 CE), with a further increase to a maximum at 5 cm (ca. 1988 CE), followed by a decline to present.

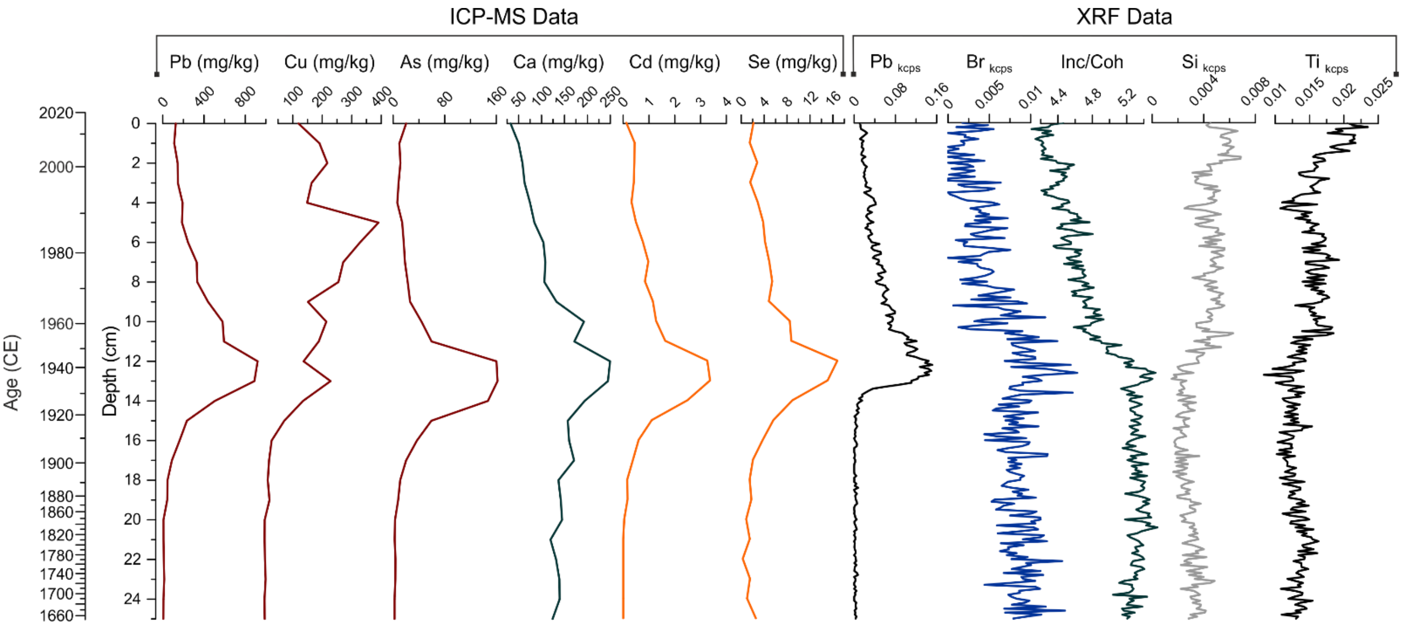

Figure 3: Stratigraphy of ICP-MS elements Pb, Cu, As, Ca, Cd, and Se in mg/kg on the left. On the right XRF elements Pb $_{kcps}$, Br $_{kcps}$, Mo Inc/Coh ratio, Si $_{kcps}$, and Ti $_{kcps}$. Extended XRF and ICP-MS results can be found in the Supplementary Data (Figs. S1 & S4).

3.3 *Charcoal and Pollen*

Charcoal accumulation is low from 25 to 18.5 cm (ca. 1654-1884 CE), followed by high accumulation from 14 cm (ca. 1927 CE) to present with maximum peaks occurring at 13 and 1.5 cm (ca. 1935 and 2004 CE) (Fig. 8h). Only two significant zones were found in the terrestrial pollen assemblages but three additional subzones were identified by breaks in the CONISS dendrogram (Fig. 4). The terrestrial pollen PCA had two significant axes, with an 11.4% explained variance for axis 1 and 9.8% for axis 2. *Eucryphia lucida*, Cupressaceae, *Nothofagus cunninghamii* (syn. *Lophozonia cunninghamii*) (Hill et al., 2015), and *Bauera rubioides* had a strong positive association with pollen PCA axis 1 and Ericaceae, *Epacris* spp., *Allocasuarina* spp., and *Monotoca* spp. had a strong negative association. Trends in the assemblage data are described by zone below (average percent abundance in parentheses):

Zone 1 [25 to 18 cm (1654 to 1892 CE)]:

In this zone, percent forest pollen is high with abundant *N. cunninghamii* (35%), *Phyllocladus aspleniifolius* (6%), *Eucalyptus* spp. (15%), *E. lucida* (4%) and Cupressaceae (2%). Near the end of this zone, *Pinus* first appears and aquatic indicators (*Botryococcus* cf. *braunii*) and pollen concentration are high while the PCA axis 1 scores are low.

Zone 2a [17.5 to 13 cm (1896 to 1935 CE)]:

Zone 2 begins with an increase in non-forest pollen. *N. cunninghamii* (25%), Cupressaceae (1.5%), and *E. lucida* (2%) are replaced by Ericaceae (20%), Poaceae (4%), and *Monotoca* spp. (6%). Pollen concentrations begin to decline and PCA axis 1 increases. *Botryococcus* reaches its maximum concentration at 16 cm (ca. 1909 CE).

Zone 2b [12.5 to 4 cm (1939 to 1992 CE)]:

Percent forest pollen decreases further in this subzone with declines in *N. cunninghamii* (15%), Cupressaceae (1%), and *E. lucida* (1%). *B. rubioides* (1%) and *Monotoca* spp. (5%) also decrease during this zone and Ericaceae (35%) and *Nothofagus gunnii* (syn. *Fuscospora gunnii*) (Hill et al., 2015) increases to a maximum abundance of 4% at 9 cm (ca. 1966 CE). PCA axis 1 has high stable values throughout the remainder of Zone 2 while pollen concentration falls to a minimum. *Botryococcus* also declines to low concentrations in this subzone.

Zone 2c [3.5 to 0 cm (1994 CE to 2015 CE)]:

This final subzone shows a decline in *N. gunnii* (2%) and Ericaceae (20%) with *Pinus* present throughout. *N. cunninghamii* and *P. aspleniifolius* recover slightly in this subzone to 25% and 10% abundance.

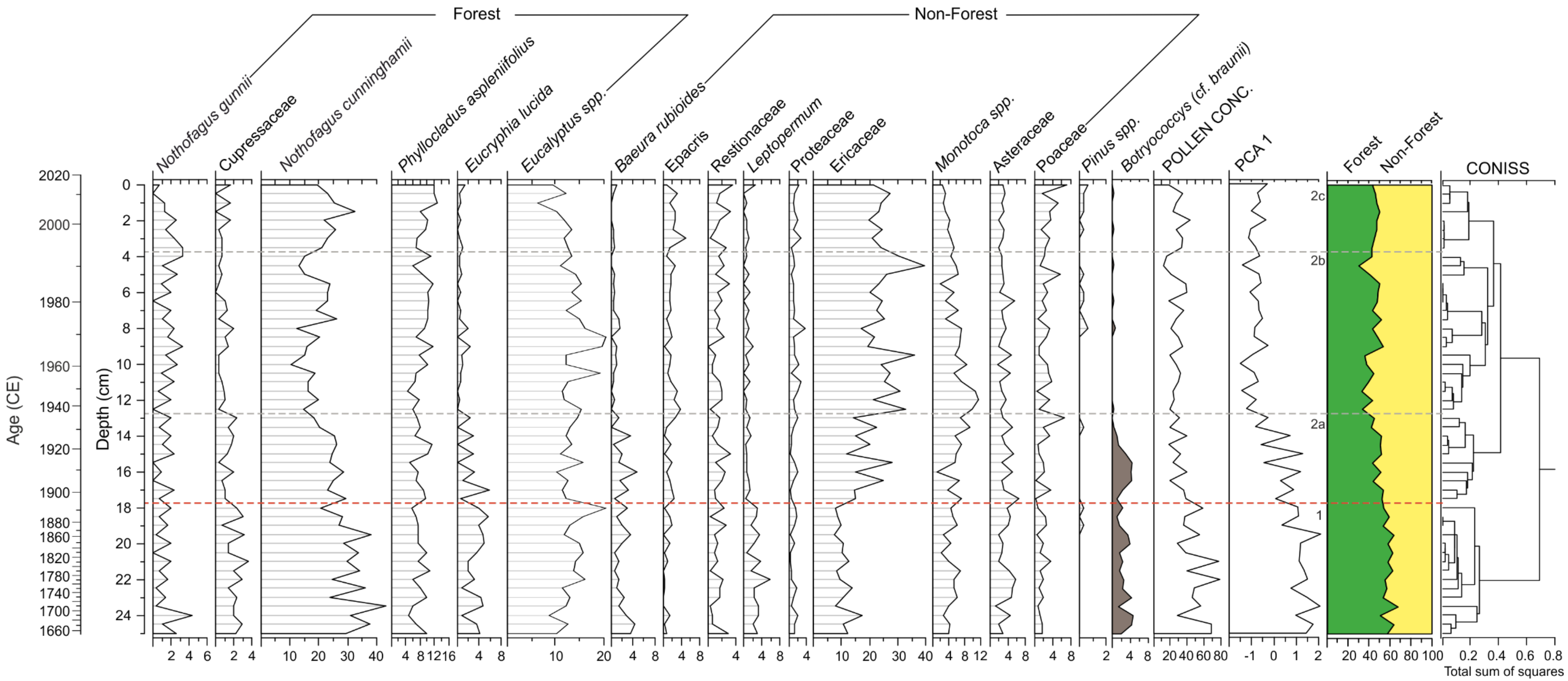

Figure 4: Terrestrial pollen stratigraphy by depth (cm) and age (CE) including pollen concentration calculated by known inputs of exotic pollen grains and pollen PCA axis 1 (explained variance of 11.4%). Two significant zones were determined (1 & 2) and three subzones (a, b, & c) using CONISS on terrestrial pollen data. Terrestrial pollen abundance was summed into two groups: forest (green), non-forest (yellow).

3.4 Diatoms

Diatoms had good preservation with 115 species identified in the top 24 cm of core TAS1501. Two significant zones were found in the diatom assemblages but four additional subzones were identified based on breaks in the CONISS dendrogram from the diatom subfossil data (Fig. 5). The diatom PCA had four significant axes with explained variances of 23.16%, 14.95%, 9.52%, and 8.69%. *Hantzschia amphioxys* and *Pinnularia divergentissima* had a strong negative association with PCA axis 1 and *Eunophora tasmanica, Eunotia praerupta, Eunotia implicata and Brachysira brebissonii* had a strong positive association. For axis 2, *Eunotia naegelii, Eunotia bilunaris, Chamaepinnularia mediocris,* and *Actinella pulchella* had strong negative associations and *Pinnularia subcapitata*, *Pinnularia subgibba*, and *Pinnularia viridis* were positively associated with PCA axis 2 (Fig. 6). For an extended diatom stratigraphy see Supplementary data (Fig. S5). Trends in the assemblage data are describe by zone below (average percent abundance in parentheses):

Zone 1a [24 to 19 cm (1689 to 1877 CE)]:

Aulacoseira distans is most abundant in this subzone, starting at a maximum abundance of 40% and declining to <1% by end of the zone. *Pinnularia viridis* (20%), *Pinnularia subgibba* (10%), and *Eunophora tasmanica* (15%) also appear in high abundance and *Eunotia denticulata* (8%), *Eunotia implicata* (4%), *Eunotia incisa* (5%), and *Pinnularia subcapitata* (2%) occur in moderate abundance. Total valve concentration and deformed:total diatom valve ratio are low during this zone.

Zone 1b [18 to 15 cm (1892 to 1917 CE)]:

Aulacoseira distans is replaced by *Brevisira arentii* (3%) during this subzone. *Pinnularia viridis* (2%), *Pinnularia subgibba* (2%), and *Eunophora tasmanica* (10%) decline and *Brachysira brebissonii* (4%), *Pinnularia subcapitata* (8%), *Eunotia paludosa* (3%), and *Eunotia* sp. 3 (4%) and sp. 5 (10%) increase in abundance. *Eunotia denticulata* (5%), *Eunotia implicata* (2%), and *Eunotia incisa* (5%) also decline during this subzone. Diatom PCA axis 1 remains high during Zone 1. Total diatom valve concentration increases to a maximum at the end of this zone (Fig. 8).

Zone 2a [14 to 1 cm (1927 to 2006 CE)]:

Zone 2 is dominated by *P. divergentissima* (30%) and *H. amphioxys* at 8%. *Eunophora tasmanica* and *Brevisira arentii* decline to <1% abundance for the remainder of the record. *Eunotia denticulata* (2%), *Eunotia implicata* (1%), and *Eunotia incisa* (2%) decline further in this subzone while *Eunotia exigua* (4%) and *E. paludosa* (6%) increase. *Discostella stelligera* (5%) appears in the middle of this subzone (10 to 4 cm, ca. 1961 to 1992 CE) then disappears. *Humidophila contenta* (4%), *Kobayasiella hodgsonii* (5%) and *Kobayasiella tasmanica* (5%) occur in their highest abundance in this subzone and diatom PCA axis 1 shifts toward low values. Total valve concentration declines back to low concentrations in this zone (Fig. 8).

Zone 2b [0.5 and 0 cm (2010 CE to2015 CE)]:

P. divergentissima and *H. amphioxys* are replaced by *Chamaepinnularia mediocris* (20%), *Eunotia naegelii* (15%), and *Actinella pulchella* (8%). *E. incisa* also increases in abundance to 15% and *E. exigua, E. denticulata* and *E. implicata* decline to low abundances (<1%). Diatom PCA axis 2 is relatively high and stable throughout this record with a sharp decline in this subzone, while PCA axis 1 shows a slight increase. Total valve concentration and the deformed:total diatom valve ratio i increase to present with a maximum in deformed valves: total valves (Fig. 8).

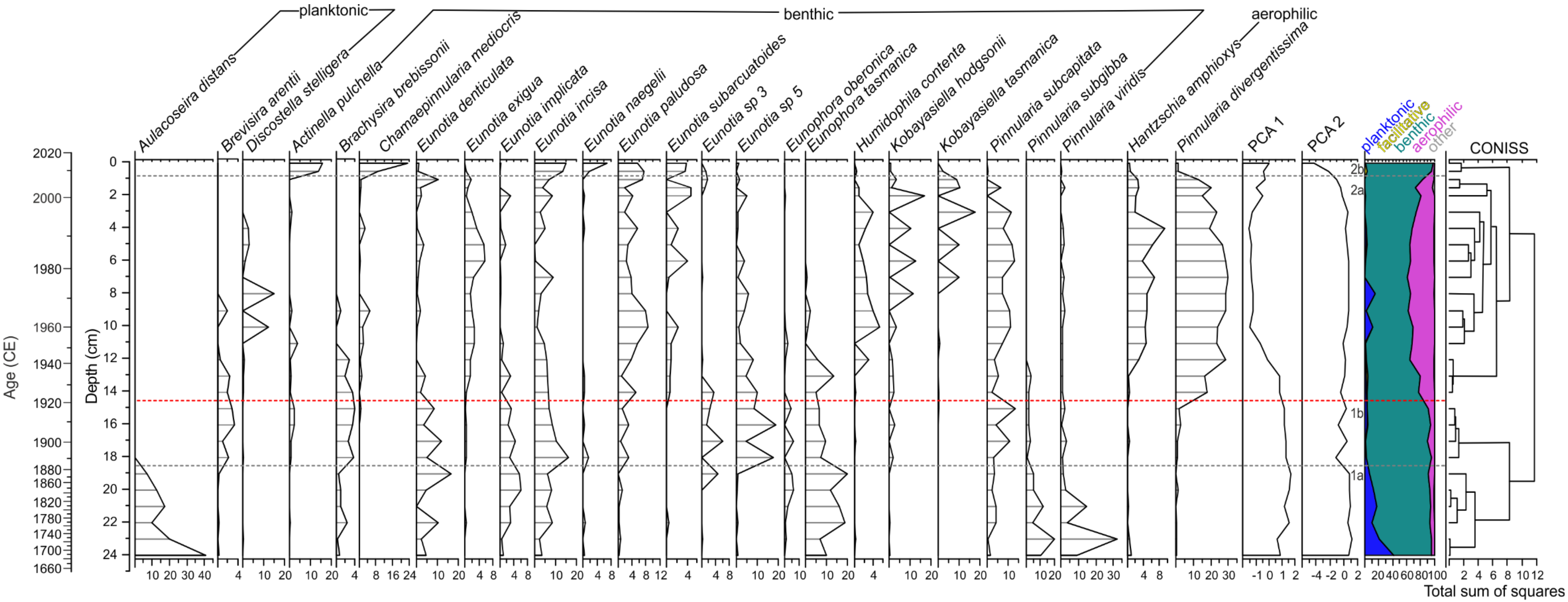

Figure 5: Stratigraphy of important diatom species by depth (cm) and age (CE) including diatom PCA axis 1 (explained variance of 23.16%) and PCA axis 2 (explained variance of 14.95%). Two significant zones (1 & 2) were determined and four subzones (a & b) using CONISS from the diatom data. Diatom species abundance were summed into groups planktonic (blue), facilitative planktonic (yellow), benthic (green), aerophilic (pink), and other (grey).

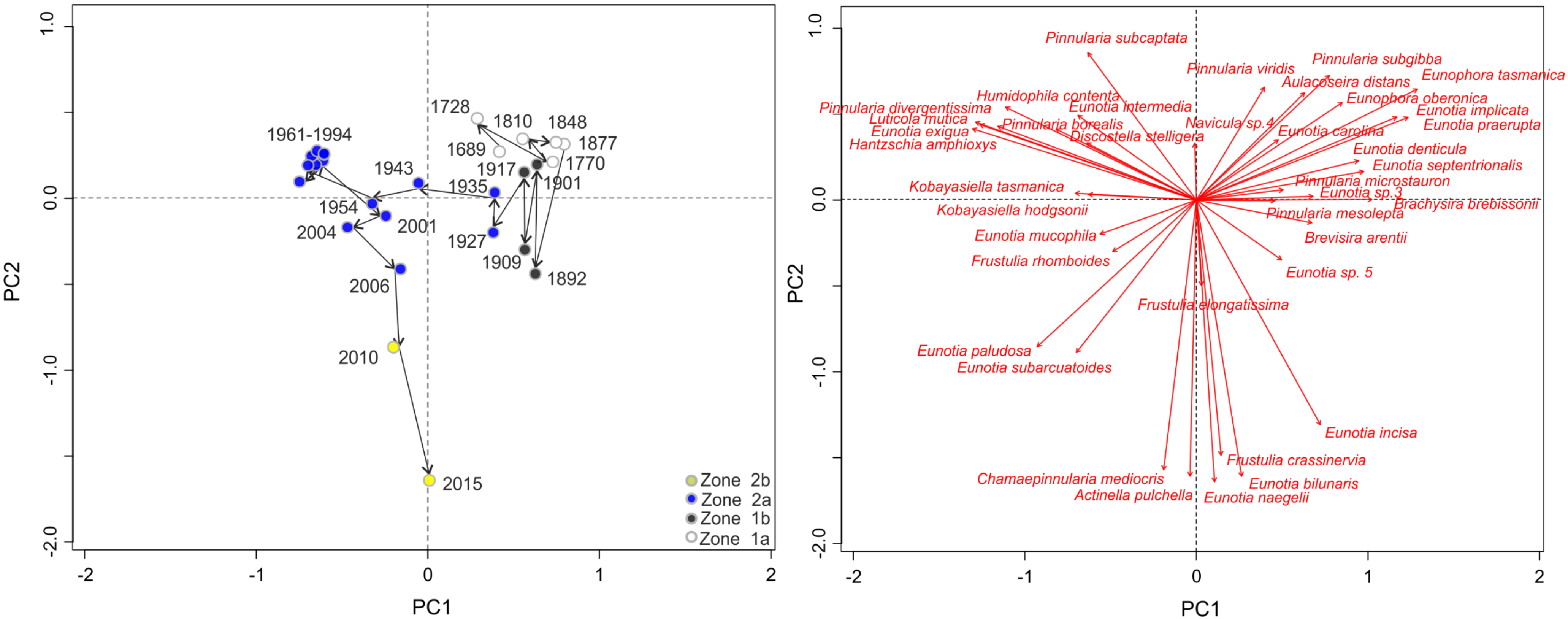

Figure 6: Diatom PCA biplot of axes 1 (variance of 23.16%) and 2 (variance of 14.95%) with depth samples by zone on the left, Zone 1a= white circles, Zone 1b=black circles, Zone 2a=blue circles, and Zone 2b=yellow circles, with arrow trajectories and ages between depth samples. On the right is the species scores of the PCA are indicated by red arrows.

3.5 Statistical analysis

GAMMs were individually fitted to the diatom PCA axis 1 and axis 2 using covariates of XRF binned data and ICP-MS data. An ANOVA was performed to determine if the covariates (geochemical proxies) were significant ($p<0.05$) predictors of the response variable (diatom PCA). Statistical results for the GAMMs can be found in Table S2 of the Supplementary data. Pb, Cu, Inc/Coh and Br all significantly explained the shifts in diatom PCA axis 1 and Ca, Inc/Coh and Ti all significantly explained the shift in diatom PCA axis 2 (Table S2). The fitted smooths of these models are found in Figure 7. The covariates (geochemistry) in the GAMM plots that diverge from the mean (dotted zero line in Fig. 7) show greater explanation of the shift in the diatom PCA curves. Therefore, Br, Cu and Inc/Coh show significant contributions to a negative shifts in diatom PCA 1 between 14-11 cm (ca. 1927-1954 CE) (Fig. 7b-d), while Pb shows a significant contribution from 16-14 cm (ca. 1909-1927 CE) and 10-6 cm (ca. 1961-1983 CE) (Fig. 7a). For diatom PCA axis 2 all covariates (Ca, Inc/Coh and Ti) show significant contributions to the negative shift in the axis scores of the uppermost depths 2 to 0 cm (ca. 2001-2015 CE) (Fig. 7 e-g).

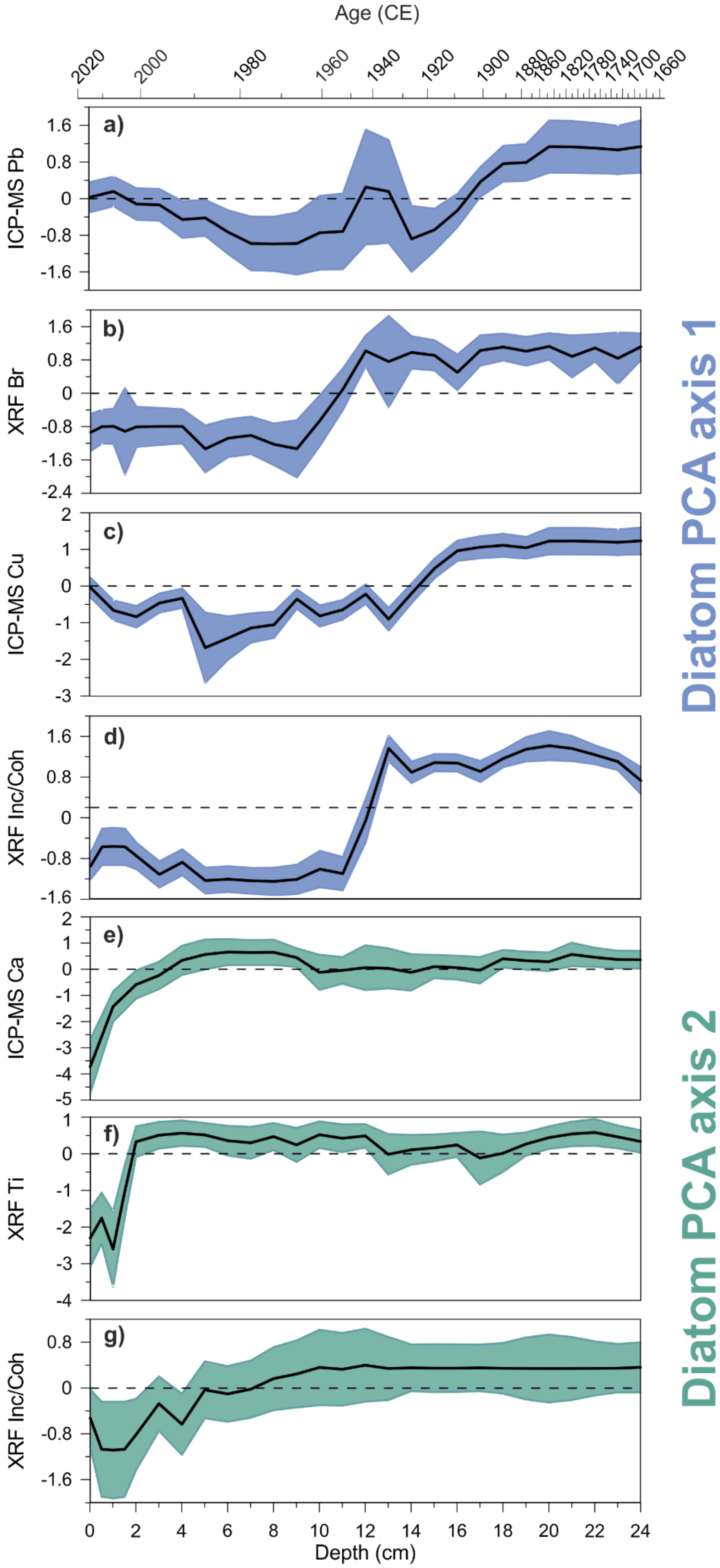

Figure 7: GAMM results for the covariates a) ICP-MS Pb (mg/kg), b) XRF Br $_{kcps}$, c) ICP-MS Cu (mg/kg), and d) XRF Inc/Coh, modelled to changes in diatom PCA axis 1 (blue) and e) ICP-MS Ca (mg/kg), f) XRF Ti $_{kcps}$, and g) XRF Inc/Coh modelled to change in diatom PCA axis 2 (green) plotted by depth (cm) and age (CE).

4. Discussion

4.1 Pre- Mining Impact Phase [24 to 19 cm (1689 to 1877 CE)]

Prior to British arrival in the late 1700s, the terrestrial landscape around Owen Tarn was characterised by a wet scrub plant community with low fire activity and high plant biomass (here interpreted from pollen concentration), with greater percentage of forest taxa (*N. cunninghamii*, Cupressaceae, and *E. lucida*; Fig. 4) consistent with a pre-mining environment. Slower sediment accumulation (Fig. 2) and high organic content (Inc/Coh and Br; Fig. 3) reflects local allochthonous carbon inputs from predominantly organic rich soils in the catchment formed under rainforest vegetation in the high rainfall landscape of western Tasmania (Wood et al., 2011). Heavy metal concentrations are low at this time in the sediment record (Fig. 3).

The diatom flora is dominated by acidic and oligotrophic taxa that are characteristic of western Tasmanian lakes (Tyler, 1992; Vyverman et al., 1995; Vyverman et al., 1996). The overall diatom community is indicative of a dystrophic lake with reasonable light availability to facilitate algal growth in the littoral environment. Additionally, the relatively high abundances of heavy siliceous planktonic diatoms (*Aulacoseira distans*) indicate either deeper mixing or longer turnover periods (Saros and Anderson, 2015). Dystrophy is indicated by the occurrence of *Eunophora tasmanica*, which has optimum gilvin and pH values of 4.434 and 4.69, respectively (Table 2) (John, 2018; Vyverman et al., 1995). A dystrophic environment with ample light penetrations is supported by the presence of *Eunotia* spp. (Bergström et al., 2000; van Dam et al., 1994; van Dam et al., 1981) and the occurrence of *P. subgibba* and *P. viridis* with a preference for littoral zones (Hodgson et al., 1996) and acidic humic lakes (Table 2) (Vyverman et al., 1995). High abundance of *Botryococcus* (cf. braunii), a eurioic algae that likes oxygenated and high conductivity environments, has a preference to littoral zones or shallow lakes (Aaronson et al., 1983; Clausing, 1999; Pinilla, 2006). The oligotrophic acidic dystrophic nature of this lake is consistent with Holocene diatom assemblages in the region before British arrival (Beck et al., 2019; Bradbury, 1986; Hodgson et al., 1996).

4.2 Early Mining Impact Phase [18 to 15 cm (1892 to 1917 CE)]

Explorative mining by the British began in the 1850s in Tasmania (Harle et al., 2002). To inspect the geological potential of the region the vegetation on the landscape was burned (Augustinus et al., 2010; Blainey, 1993; Bottrill, 2000; Harle et al., 2002; Keele, 2003). An increase in charcoal at 19.5 cm (ca. 1863 CE) is believed to be the early impacts of mining (Fig. 8h). Ore production and smelting processes required large amounts of fuel harvested from the region (McQuade et al., 1995). The start of smelting is consistent with a decline in forest pollen (Fig. 8d) and pollen concentration, and an increase in Ericaceous shrubs (Fig. 4). An increase in sedimentation (Fig. 2) and heavy metals (Fig. 3) at this time indicate changing environmental conditions from pre-mining impact to landscape clearing and early mining.

The complex diatom ecology during this period is indicative of landscape disturbance from the early impacts of mining. The combination of dystrophic (*Eunophora tasmanica, Eunotia spp., B. brebissonii*) (John, 2018), mesotrophic planktonic (*B. arentii*) (Fernández et al., 2012), and benthic taxa (*B. brebissonii* and *P. subcapitata*) and the loss of heavy planktonic *A. distans* indicate more terrestrial material coming into the lake (Norbäck Ivarsson et al., 2013). Western Tasmania is blanketed in peats (Brown et al., 1982; Tyler, 1974) and increases in fire and erosion have shown to decrease light availability via increased humic stain (from peat inputs) and/or erosion of terrigenous material (Beck et al., 2019; Mariani et al., 2018). Such conditions could favour both dystrophic and mesotrophic taxa. Further, increased inputs from surrounding blanket peats would include organic compounds and nutrients providing favourable conditions for diatoms to flourish (maximum diatom valves; Fig. 8e). However, as sedimentation accelerates, and peat is removed from the landscape and not replaced, material entering the lake would decline in available nutrients and increase in inorganic content, limiting light availability and impeding algal growth, i.e. valve concentration decreases at 14 cm (ca. 1927 CE) (Fig. 8e). Therefore, our diatom proxy data suggests the early influence of British settlement and mining on the terrestrial and aquatic environment.

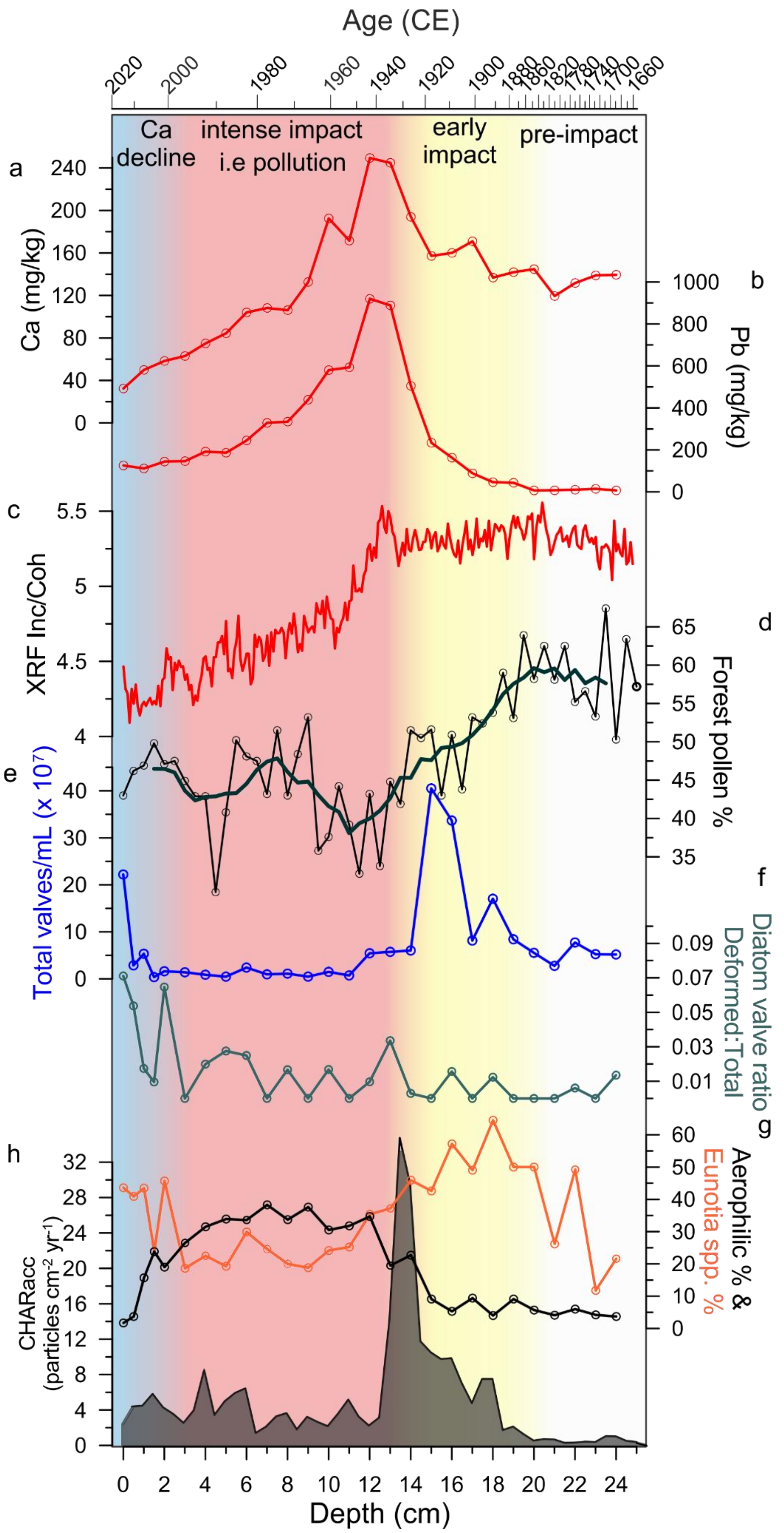

Figure 8: Summary figure of mining impact at Owen Tarn. A) ICP-MS Ca concentration (mg/kg), b) ICP-MS Pb concentration (mg/kg), c) XRF Inc/Coh ratio, d) total percent forest pollen, e) total diatom valve concentration/mL ($x10^7$) in blue, f) deformed:total diatom valve ratio in green, g) total percent aerophilic diatoms in black and *Eunotia* spp. in orange, and h) macroscopic charcoal accumulation rate (particles cm^{-2} yr^{-1}) in grey.

4.3 Intense Mining Impact Phase [14 to 1 cm (1927 to 2006 CE)]

Mt. Lyell Co. mining activities were initially underground; however, due to a decline in ore quality open-cut mining expanded in operation (McQuade et al., 1995). A peak in charcoal accumulation at 13.5 cm (ca. 1931 CE) followed by drop in charcoal is consistent with a shift from timber and coal fuelled smelting to floatation technology in 1922 CE when high-grade ore deposits were depleted. By the 1930s Mt. Lyell mining sites expanded their open-cut operations resulting in maximum ore production and tailings waste until 1980 CE (McQuade et al., 1995). Peak in mining activity, both due to new ore processing methods and large scale production, is apparent in the Owen Tarn record at 14-12 cm (ca. 1927-1943 CE) with the highest concentrations of heavy metals (Fig. 3) and peak charcoal accumulation (Fig. 8h). Consistent with nearby studies in western Tasmania, Macquarie Harbour ~ 40 km from Owen Tarn (Augustinus et al., 2010) and Lake Dora ~ 20 km (Harle et al., 2002). Peak in heavy metal concentration is simultaneous with a further decline in forest pollen, increase in the proportion of Ericaceae pollen, and reduction in the total pollen concentration, indicating an overall decrease in plant biomass within the catchment (Fig. 8d). The loss of vegetation and organic soils from the catchment resulted in a reduction of organic matter input into the tarn as inorganic sedimentation increased (Si and Ti; Fig. 3).

The drastic change in the landscape had significant impacts on the diatom community. *Eunotia* spp., found in oligotrophic and dystrophic environments, were replaced by aerophilic taxa, *P. divergentissima* and *H. amphioxys*. Aerophilic taxa are tolerant of harsh and stressful environments, such as moisture stress, air exposure and high sedimentation or erosion (Leahy et al., 2005; Norbäck Ivarsson et al., 2013; Smol and Stoermer, 2010). Hodgson et al. (2000) originally suggested this assemblage was the less acidic environment prior to mining; however, our findings suggest this period is, in fact, the period of intensive mining impact. During this period there is no obvious change in acidity (Table 2), but the dominance of species tolerant of trace metal contamination (Maznah and Mansor, 2002), and high sedimentation (Kawecka and Olech, 1993; Leahy et al., 2005; Van de Vijver et al., 2013) suggests impacts of high sediment loading and environmental stress. GAMM results corroborate these findings. A decline in the diatom PCA axis 1 between 14 to 12 cm (ca. 1927-1943 CE) is significantly explained by changes in the organic matter indicators and heavy metals

(Fig. 7). This shift is represented by a migration of the PCA axis 1 into negative values affiliated with aerophilic diatoms (*H. amphioxys* and *P. divergentissima*) (Fig. 6).

By the 1980s, mining began to decline and by 1994 CE the Mt. Lyell Co. mine closed (Teasdale et al., 2003). Around 1995 CE in the Owen Tarn record, heavy metals had fallen to low concentrations. Declines in charcoal accumulation from 12 to 6 cm (ca. 1943-1983 CE) are consistent with a slight recovery in the forest vegetation (Fig. 8d), suggesting a decline in mining activity. However, the diatom record appears stable with an impacted assemblage until ca. 2001 CE, with the exception of a decline in *H. amphioxys* at 4 cm (ca. 1992 CE). The PCA values suggest the diatom community is far away from its baseline conditions between 1961 to 1994 CE and, therefore, remains strongly impacted even after mining has ceased (Fig. 6). This is likely due to the largely lunar landscape at Owen Tarn and continued high sedimentation of terrigenous material to present. Around 1995 CE, forest pollen recovers further consistent with the final fall in the aerophilic diatoms (Fig. 8g).

4.4 Post Mining Impact Phase [0.5 and 0 cm (2010 CE to 2015 CE)]

The aquatic environment from ca. 2010-2015 CE suggests an acidic oligotrophic environment (*E. naegelii*, *C. mediocris*, and *Actinella* spp.), typical of western Tasmanian lakes pre-mining. However, this assemblage is different from the pre-impact assemblage and does not appear to be in a recovery state (Fig. 6). GAMM results show that the most recent shift in diatom PCA axis 2 can be explained by inorganic indicators (Inc/Coh and Ti), and Ca. Ca is on the decline since 12 cm (ca. 1943 CE) based on sediment geochemical data but only decreases below the pre-mining concentrations at 8 cm (ca. 1972 CE).

Low Ca is apparent across temperate soft water lakes impacted by mining. Initial acid deposition (S and NOx) will release Ca, then, over time, Ca is leached from the catchment and not replaced, irrespective of changes in pH (Jeffries et al., 2003; Keller et al., 2001). This is further exacerbated by loss of terrestrial biomass which can replenish base cation stocks in catchments (Saikh et al., 1998). Ca declines are consistent with other findings in the western Tasmanian region. Reduced Ca content was also found in the tailing deposits of Macquarie Harbour (Augustinus et al., 2010). They described a shift toward lower Ca content as an indicator of low tailings pollution; however, their findings also show the Ca content post mining is lower than background conditions suggesting a potential regional Ca decline from mining. This decline in Ca concentrations of freshwaters can have consequences for the aquatic biota (Cairns and Yan, 2009; Edwards et al., 2015; Jeziorski et al., 2008).

Ca is an important salt for freshwater organisms, such as zooplankton that use calcium carbonate to form their carapaces (Barrow et al., 2014; Jeziorski and Yan, 2006; Jeziorski et al., 2008). Declines in Ca have shown direct impacts to zooplankton biomass, which can disrupt the trophic linkages with phytoplankton (Arnott et al., 2017; Burns and Schallenberg, 1996; Nevalainen et al., 2014; Winder and Schindler, 2004). At Owen Tarn, an increase in total diatom valve concentration in the recent sediments (Fig. 8e) may be related to less predation from a declining zooplankton population. However, the unique diatom assemblage and peak number of deformed valves at this time indicates the diatoms may also be experiencing the direct effects of Ca decline (Fig. 8f). Diatoms require Ca for inter and extracellular mechanisms such as mobility and adhesion, biogenesis of silica cell walls, and anchoring cell membranes to cell walls (Geesey et al., 2000; Strynadka and James, 1989). The dominant diatom taxa (*Actinella* spp. *C. mediocris, E. naegelli, E. incisa and E. paludosa*) during this period have lower Ca optima and tolerance than the other species in previous zones (Table 2) (Vyverman et al., 1995; Vyverman et al., 1996). These species are also considered to be less motile (Diatoms of North America, 2019) potentially reflecting their tolerance for lower Ca environments. Therefore, the combination of evidence from increased valve concentrations, a unique assemblage tolerant of low Ca, and peak values in deformed diatom valves suggest the aquatic environment at Owen Tarn is experiencing the effects of Ca declines and has not fully recovered from mining activity.

Table 2: Table of Ca, gilvin and pH tolerances of diatom taxa determined and adapted from Vyverman et al. (1995); Vyverman et al. (1996) in order of low to high Ca optimum. Tol.= tolerance. Opt.= optimum. This data was collected for the TASDIAT training set from 76 lakes in Tasmania from 1994-1995. Data was used to explore the main trends in the water chemistry data and diatom species using a PCA ordination analysis.

Species	pH opt.	pH tol.	Ca opt.	Ca tol.	Gilvin opt.	Gilvin tol.
Eunotia septentrionalis	4.32	0.59	19.37	11.37	6.118	2.556

Actinella indistincta	4.95	0.93	25.68	12.22	5.511	5.138
Chamaepinnularia mediocris	4.7	0.77	26.1	19.6	4.272	2.684
Eunotia naegelii	4.94	0.91	26.23	18.29	5.221	3.863
Eunotia incisa	4.76	0.83	26.5	21.01	6.139	3.714
Eunophora sp.	4.69	0.76	26.6	21.6	4.434	2.751
Eunotia exigua	4.93	1.05	28.49	19.31	5.322	4.028
Eunotia paludosa	5.19	0.96	28.5	15.27	3.192	3.272
Pinnularia viridis	5.66	0.96	31.1	17.3	1.791	2.507
Brevisira arentii	4.94	0.94	33.65	35.01	4.730	2.868
Actinella tasmaniensis	5.8	0.76	33.84	9.9	-	-
Eunotia bilunaris	5.59	0.84	34.42	16.93	-	-
Brachysira brebissonii	5.48	0.92	35.7	26.5	2.116	2.604
Kobayasiella hodgsonii	5.4	0.91	40.56	29.55	2.552	3.426
Pinnularia subcapitata	5.62	0.92	41	29.9	1.834	2.933
Brachysira styriaca	5.82	0.67	45.21	31.16	1.019	1.768
Aulacoseira distans	5.44	0.76	45.64	28.63	2.215	2.417
Pinnularia gibba	5.31	0.93	45.8	31.7	2.713	2.840
Brachysira microcephala	5.65	0.62	59.96	44.13	-	-
Discostella stelligera	5.78	0.51	77.46	50.38	1.022	0.827

5. Conclusions and Future Research

Our findings from the Owen Tarn multiproxy palaeoecological study found four key phases of mining impact: 1) pre-mining, 2) early mining, 3) intense mining, and 4) post- mining. The results from these phases allow us to address our research questions.

1) *What are the aquatic ecosystem baseline conditions at Owen Tarn?*

   Low heavy metals (Cu, Pb, Cd, and Se), high organic content (Inc/Coh), slow sedimentation, low fire activity, and high biomass (forest pollen) were characteristic of the environment before mining. Pre-mining conditions are mirrored in the diatom assemblage with species characteristic of an oligotrophic acidic dystrophic lake and sufficient light availability, typical of western Tasmanian lakes pre- British arrival.

2) *Was the aquatic and terrestrial environment impacted by mining? If so how?*

Our results suggest sediment pollution caused by mining had the greatest impact on the diatom community. In the late 1800s, mining began in western Tasmania due of the abundant ore deposits in the region. Increases in dystrophic and mesotrophic taxa during this period indicate allochthonous inputs and low light environments from early mining. Deforestation was required to fuel smelting practices resulting in high charcoal, reduced biomass (decline in forest pollen) and increased erosion. By the 1930s, Mt. Lyell was intensely mined resulting in peak heavy metal (Pb, Cu, As, Se and Cd) concentration consistent with the height of mining efficiency from 1930-1980 CE. A peak in charcoal and decline in forest pollen suggest extensive clearing from mining. This intensive mining caused low diatom productivity and dominant aerophilic diatom taxa (*H. amphioxys* and *P. divergentissima*), tolerant of metal pollution and sediment deposition.

3) *Has the aquatic biota and local vegetation recovered to pre-disturbance conditions since the Mt. Lyell mine closed ?*

While vegetation biomass and heavy metal concentration has shown some recovery from mining activity, no obvious recovery has been detected in the aquatic environment after mining has ceased. The most recent diatom assemblage at Owen Tarn (dominant *E. naegalii*, *C. mediocris* and *Actinella* spp.) does not show overlap or trajectories toward pre-mining ecological conditions, but rather secondary impacts of Ca decline.

When restoring impacted environments it is vital to know baseline conditions so management strategies can aim toward pre-impact environment. At Owen Tarn, we observed an aquatic environment that was severely impacted by sediment loading and heavy metal pollution followed by secondary impacts post-mining where the aquatic environment moved towards a different diatom assemblage to pre-mining conditions. Therefore, palaeoenvironmental reconstructions are crucial to inform conservation and restoration management toward appropriate targets.

6. Acknowledgements

This project was financially supported by the Australian Research Council (award: DI110100019 and IN140100050) and the Australian Institute of Nuclear Science and Engineering (AINSE – award ALNGRA16/024). Michela Mariani would like to acknowledge the support of the AINSE Postgraduate Research Award #12039. We would like to thank Tasmania National Parks and Wildlife Service and the Traditional Owners both past and present for their support in allowing us to work on their lands. Kristen K. Beck would like to acknowledge the Albert Shimmins Fund for their financial support. We would also like to thank Scott Nichols, Stella Thomas and Kilian Thomas for their assistance in the field and Gavin L. Simpson for his help with the statistical analyses. The data from this manuscript will be made publicly available on Neotoma (https://www.neotomadb.org/) upon date of publication. We would also like to thank the anonymous reviewers for the helpful feedback on this work.

References:

Aaronson, S., Berner, T., Gold, K., Kushner, L., Patni, N., Repak, A., Rubin, D., 1983. Some observations on the green planktonic alga, *Botryococcus braunii* and its bloom form. Journal of Plankton Research 5, 693-700.

Andrade, C.F., Jamieson, H.E., Kyser, T.K., Praharaj, T., Fortin, D., 2010. Biogeochemical redox cycling of arsenic in mine-impacted lake sediments and co-existing pore waters near Giant Mine, Yellowknife Bay, Canada. Applied Geochemistry 25, 199-211.

Aquino-López, M.A., 2018. Plum for ^{210}Pb chronologies, Plum for ^{210}Pb chronologies, 0.1.0 ed, pp. Plum is an apporach to ^{210}Pb age-depth modelling that uses Bayesian statistics (https://doi.org/^{2}10.1007/s13253-13018-10328-13257).

Aquino-López, M.A., Blaauw, M., Christen, J.A., Sanderson, N.K., 2018. Bayesian Analysis of ^{210}210Pb Dating. Journal of Agricultural, Biological and Environmental Statistics 23, 317-333.

Arnott, S., Azan, S., Ross, A., 2017. Calcium decline reduces population growth rates of zooplankton in field mesocosms. Canadian Journal of Zoology 95, 323-333.

Arseneau, K.M., Driscoll, C.T., Brager, L.M., Ross, K.A., Cumming, B.F., 2011. Recent evidence of biological recovery from acidification in the Adirondacks (New York, USA): a multiproxy paleolimnological investigation of Big Moose Lake. Canadian Journal of Fisheries and Aquatic Sciences 68, 575-592.

Augustinus, P., Barton, C.E., Zawadzki, A., Harle, K., 2010. Lithological and geochemical record of mining-induced changes in sediments from Macquarie Harbour, southwest Tasmania, Australia. Environmental Earth Science 61, 625-639.

Barrow, J.L., Jeziorski, A., Rühland, K.M., Hadley, K.R., Smol, J.P., 2014. Diatoms indicate that calcium decline, not acidification, explains recent cladoceran assemblage changes in south-central Ontario softwater lakes. Journal of Paleolimnology 52, 61-75.

Battarbee, R., Flower, R., Stevenson, A., Jones, V., Harriman, R., Appleby, P., 1988. Diatom and chemical evidence for reversibility of acidification of Scottish lochs. Nature 332, 530-532.

Battarbee, R.W., 1984. Diatom analysis and the acidification of lakes. Philosophical Transactions of the Royal Society of London. B, Biological Sciences 305, 451-477.

Battarbee, R.W., 1986. Diatom analysis, in: Berglund, B.E. (Ed.), Handbook Palaeoecology and Palaeohydrology. John Wiley & Sons, Chichester, pp. 527-570.

Beck, K.K., Fletcher, M.S., Gadd, P., Heijnis, H., Saunders, K.M., Zawadzki, A., 2019. The long-term impacts of climate and fire on catchment processes and aquatic ecosystem response in Tasmania, Australia. Quaternary Science Reviews 221, 105892.

Bergström, A.-K., Jansson, M., Blomqvist, P., Drakare, S., 2000. The influence of water colour and effective light climate on mixotrophic phytoflagellates in three small Swedish dystrophic lakes. Internationale Vereinigung für theoretische und angewandte Limnologie: Verhandlungen 27, 1861-1865.

Bertrand, S., Araneda, A., Vargas, P., Jana, P., Fagel, N., Urrutia, R., 2012. Using the N/C ratio to correct bulk radiocarbon ages from lake sediments: insights from Chilean Patagonia. Quaternary Geochronology 12, 23-29.

Blainey, G., 1993. The peaks of Lyell. St. David's Park Publishing, Hobart, Tasmania.

Bottrill, R., 2000. Tasmanian Geological SurveyRecord 2001/08: A Mineralogical Field Guide for the Western Tasmania Minerals and Museums Tour, Mineral Resources Tasmania, Tasmania.

Bowman, D.M.J.S., Balch, J., Artaxo, P., Bond, W.J., Cochrane, M.A., D'Antonio, C.M., DeFries, R., Johnston, F.H., Keeley, J.E., Krawchuk, M.A., Kull, C.A., Mack, M., Moritz, M.A., Pyne, S., Roos, C.I., Scott, A.C., Sodhi, N.S., Swetnam, T.W., 2011. The human dimension of fire regimes on Earth. Journal of Biogeography 38, 2223-2236.

Bradbury, P.J., 1986. Late Pleistocene and Holocene paleolimnology of two mountain lakes in western Tasmania. PALAIOS 1, 381-388.

Brown, M.J., Crowden, R.K., Jarman, S.J., 1982. Vegetation of an alkaline pan — acidic peat mosaic in the Hardwood River Valley, Tasmania. Australian Journal of Ecology 7, 3-12.

Buckney, R., Tyler, P., 1973. Chemistry of some sedgeland waters: Lake Pedder, south-west Tasmania. Australian Journal of Marine and Freshwater Research 24, 267-273.

Burns, C.W., Schallenberg, M., 1996. Relative impacts of copepods, cladocerans and nutrients on the microbial food web of a mesotrophic lake. Journal of Plankton Research 18, 683-714.

Cairns, A., Yan, N., 2009. A review of the influence of low ambient calcium concentrations on freshwater daphniids, gammarids, and crayfish. Environmental Reviews 17, 67-79.

Clausing, A., 1999. Palaeoenvironmental significance of the green alga Botryococcus in the lacustrine rotliegend (upper carboniferous-lower permian). Historical Biology 13, 221-234.

Corbett, K.D., 2001. New mapping and interpretations of the Mount Lyell mining district, Tasmania: a large hybrid Cu-Au system with an exhalative Pb-Zn top. Economic Geology 96, 1089-1122.

Croudace, I.W., Rothwell, R.G., 2015. Micro-XRF Studies of Sediment Cores: Applications of a non-destructive tool for the environmental sciences. Springer Science + Business Media Dordrecht, Dordrecht Heidelberg New York London.

Diatoms of North America, 2019. Diatoms of North America: The source for diatom identification and ecology. United States Environmental Protection Agency, United States.

Edwards, B.A., Jackson, D.A., Somers, K.M., 2015. Evaluating the effect of lake calcium concentration on the acquisition of carapace calcium by freshwater crayfish. Hydrobiologia 744, 91-100.

Faegri, K., Iversen, J., 1989. Textbook of pollen analysis, 4 ed. John Wiley & Sons Ltd., London, Great Britain.

Fedotov, A., Trunova, V., Enushchenko, I., Vorobyeva, S., Stepanova, O., Petrovskii, S., Melgunov, M., Zvereva, V., Krapivina, S., Zheleznyakova, T., 2015. A 850-year record climate and vegetation changes in East Siberia (Russia), inferred from geochemical and biological proxies of lake sediments. Environmental earth sciences 73, 7297-7314.

Fernández, M., Maidana, N., Rabassa, J., 2012. Palaeoenvironmental conditions during the Middle Holocene at Isla de los Estados (Staaten Island, Tierra del Fuego, 54° S, Argentina) and their influence on the possibilities for human exploration. Quaternary International 256, 78-87.

Field, E., Tyler, J., Gadd, P.S., Moss, P., McGowan, H., Marx, S., 2018. Coherent patterns of environmental change at multiple organic spring sites in northwest Australia: Evidence of Indonesian-Australian summer monsoon variability over the last 14,500 years. Quaternary Science Reviews 196, 193-216.

Findlay, D.L., 2003. Response of Phytoplankton Communities to Acidification and Recovery in Killarney Park and the Experimental Lakes Area, Ontario. AMBIO: A Journal of the Human Environment 32, 190-195.

Geesey, G., Wigglesworth-Cooksey, B., Cooksey, K.E., 2000. Influence of calcium and other cations on surface adhesion of bacteria and diatoms: A review. Biofouling 15, 195-205.

Graham, M.D., Vinebrooke, R.D., Keller, B., Heneberry, J., Nicholls, K.H., Findlay, D.L., 2007. Comparative responses of phytoplankton during chemical recovery in atmospherically and experimentally acidified lakes. Journal of Phycology 43, 908-923.

Grimm, E.C., 1987. CONISS: a FORTRAN 77 program for stratigraphically constrained cluster analysis by the method of incremental sum of squares. Computers & Geosciences 13, 13-35.

Harle, K.J., Britton, K., Heijnis, H., Zawadzki, A., Jenkinson, A.V., 2002. Mud, mines and rainforest: a short history of human impact in western Tasmania, using pollen, trace metals and lead-210. Australian Journal of Botany 50, 481-497.

Hill, R.S., Jordan, G.J., Macphail, M.K., 2015. Why we should retain Nothofagus sensu lato. Australian Systematic Botany 28, 190-193.

Hodgson, D., Tyler, P., Vyverman, W., 1996. The palaeolimnology of Lake Fidler, a meromictic lake in south-west Tasmania and the significance of recent human impact. Journal of Paleolimnology 18, 313-333.

Hodgson, D.A., Vyverman, W., Chepstow-Lusty, A., Tyler, P.A., 2000. From rainforest to wasteland in 100 years: The limnological legacy of the Queenstown mines, Western Tasmania. Archiv fur Hydrobiologie 146, 153-176.

Jeffries, D., Brydges, T., Dillon, P., Keller, W., 2003. Monitoring the results of Canada/USA acid rain control programs: some lake responses. Environmental Monitoring and Assessment 88, 3-19.

Jeziorski, A., Yan, N.D., 2006. Species identity and aqueous calcium concentrations as determinants of calcium concentrations of freshwater crustacean zooplankton. Canadian Journal of Fisheries and Aquatic Sciences 63, 1007-1013.

Jeziorski, A., Yan, N.D., Paterson, A.M., DeSellas, A.M., Turner, M.A., Jeffries, D.S., Keller, B., Weeber, R.C., McNicol, D.K., Palmer, M.E., McIver, K., Arseneau, K., Ginn, B.K., Cumming, B.F., Smol, J.P., 2008. The Widespread Threat of Calcium Decline in Fresh Waters. Science 322, 1374-1377.

John, J., 2018. Diatoms of Tasmania: Taxonomy and Biogeography. Koeltz Botanical Books, Kapellenbergstr.

Juggins, S., 2018. Package 'rioja', Analysis of Quaternary Science Data, 0.9-15.1 ed, pp. Functions for the analysis of Quaternary science data, including constrained clustering, WA, WAPLS, IKFA, MLRC and MAT transfer functions, and stratigraphic diagrams.

Kaasalainen, M., Yli-Halla, M., 2003. Use of sequential extraction to assess metal partitioning in soils. Environmental Pollution 126, 225-233.

Kawecka, B., Olech, M., 1993. Diatom communities in the Vanishing and Ornithologist Creek, King George Island, South Shetlands, Antarctica. Hydrobiologia 269/270, 327-333.

Keele, S., 2003. LUNAR LANDSCAPES AND SULPHUROUS SMOGS: An environmental history of human impacts on the Queenstown region in western Tasmania c.1890-2003, School of Anthropology, Geography and Environmental Studies. University of Melbourne, Parkville, Victoria, p. 140.

Keller, W., Dixit, S., Heneberry, J., 2001. Calcium declines in northeastern Ontario lakes. Canadian Journal of Fisheries and Aquatic Sciences 58, 2011-2020.

Keller, W., Gunn, J., Yan, N., 1992. Evidence of biological recovery in acid-stressed lakes near Sudbury, Canada. Environmental Pollution 78, 79-85.

Keller, W.B., Gunn, J.M., Yan, N.D., 1998. Acid rain—perspectives on lake recovery. Journal of Aquatic Ecosystem Stress and Recovery 6, 207-216.

Knighton, A.D., 1989. River adjustment to changes in sediment load: The effects of tin mining on the Ringarooma River, Tasmania, 1875–1984. Earth Surface Processes and Landforms 14, 333-359.

Kopáček, J., Hejzlar, J., Kaňa, J., Norton, S.A., Stuchlík, E., 2015. Effects of Acidic Deposition on in-Lake Phosphorus Availability: A Lesson from Lakes Recovering from Acidification. Environmental Science & Technology 49, 2895-2903.

Leahy, P.J., Tibby, J., Kershaw, A.P., Heijnis, H., Kershaw, J.S., 2005. The impact of European settlement on Bolin Billabong, a Yarra River floodplain lake, Melbourne, Australia. River Research and Applications 21, 131-149.

Maher, W., Forster, S., Krikowa, F., Snitch, P., Chapple, G., Craig, P., 2001. Measurement of trace elements and phosphorus in marine animal and plant tissues by low-volume microwave digestion and ICP-MS. Atomic Spectroscopy 22, 361-370.

Mariani, M., Beck, K.K., Fletcher, M.S., Gell, P., Saunders, K.M., Gadd, P., Chisari, R., 2018. Biogeochemical responses to Holocene hydroclimate fluctuations in the Tasmanian World Heritage Area, Australia. Journal of Geophysical Research Biogeosciences 123, 1610-1624.

Mariani, M., Fletcher, M.-S., Haberle, S., Chin, H., Zawadzki, A., Jacobsen, G., 2019. Climate change reduces resilience to fire in subalpine rainforests. Global Change Biology 25, 2030-2042.

Maznah, W.O.W., Mansor, M., 2002. Aquatic pollution assessment based on attached diatom communitiesin the Pinang River Basin, Malaysia. Hydrobiologia 487, 229-241.

McMinn, A., Augustinus, P., Alcheringa, B.C., 2003. Diatom analysis of late Holocene sediment cores from Macquarie Harbour, Tasmania. Alcheringa 27, 135-153.

McQuade, C.V., Johnston, J.F., Innes, S.M., 1995. Mount Lyell Remediation: Review of Historical Literature and Data on the Sources and Quality of Effluent from the Mount Lyell Lease Site, in: Management, D.o.E.a.L. (Ed.). Supervising Scientist and Department of Environment and Land Management, Tasmania, Australia.

Mills, K., Schillereff, D., Talbot, É., Gell, P., Anderson, J.N., Arnaud, F., Dong, X., Jones, M., McGowan, S., Massaferro, J., Moorhouse, H., Perez, L., Ryves, D., B., 2017. Deciphering long term records of natural variability and human impact as recorded in lake sediments: a palaeolimnological puzzle. Wiley Interdisciplinary Reviews: Water 4, 1195.

National Vegetation Information System, 2018a. Major Vegetation Groups – Estimated Pre- 1750 Vegetation Version 5.1, in: Energy, D.o.E.a. (Ed.). Australian Government, Australia.

National Vegetation Information System, 2018b. Major Vegetation Groups – Extant Vegetation Version 5.1, in: Energy, D.o.E.a. (Ed.). Australian Government, Australia.

Nevalainen, L., Ketola, M., Korosi, J.B., Manca, M., Kurmayer, R., Koinig, K.A., Psenner, R., Luoto, T.P., 2014. Zooplankton (Cladocera) species turnover and long-term decline of Daphnia in two high mountain lakes in the Austrian Alps. Hydrobiologia 722, 75-91.

Norbäck Ivarsson, L., Ivarsson, M., Lundberg, J., Sallstedt, T., Rydin, C., 2013. Epilithic and aerophilic diatoms in the artificial environment of Kungsträdgården metro station, Stockholm, Sweden. International Journal of Speleology 42, 289-297.

Norris, R.H., Lake, P.S., 1984. Trace metal concentrations in fish from the South Esk River, northeastern Tasmania, Australia. Bulletin of Environmental Contamination and Toxicology 33, 348-354.

Oksanen, J., Blanchet, F.G., Kindt, R., Legendre, P., Minchin, P.R., O'Hara, R.B., Simpson, G.L., Solymos, P., Stevens, M.H.H., Wagner, H., 2019. package: vegan, Community Ecology Package, 2.5-4 ed, pp. Ordination methods, diversity analysis and other functions for community and vegetation ecologists.

Pinilla, G.A., 2006. Vertical distribution of phytoplankton in a clear water lake of Colombian Amazon (Lake Boa, Middle Caquetá). Hydrobiologia 568, 79-90.

Saikh, H., Varadachari, C., Ghosh, K., 1998. Effects of deforestation and cultivation on soil CEC and contents of exchangeable bases: a case study in Simlipal National Park, India. Plant and Soil 204, 175-181.

Saros, J.E., Anderson, N.J., 2015. The ecology of the planktonic diatom Cyclotella and its implications for global environmental change studies. Biological Reviews 90, 522-541.

Saunders, K.M., Harrison, J.J., Butler, E.C.V., Hodgson, D.A., McMinn, A., 2013. Recent environmental change and trace metal pollution in World Heritage Bathurst Harbour, southwest Tasmania, Australia. Journal of Paleolimnology 50, 471-485.

Schneider, L., Mariani, M., Saunders, K.M., Maher, W.A., Harrison, J.J., Fletcher, M.-S., Zawadzki, A., Heijnis, H., Haberle, S.G., 2019. How significant is atmospheric metal contamination from mining activity adjacent to the Tasmanian Wilderness World Heritage Area? A spatial analysis of metal concentrations using air trajectories models. Science of The Total Environment 656, 250-260.

Seen, A., Townsend, A., Atkinson, B., Ellison, J., Harrison, J., Heijnis, H., 2004. Determining the history and sources of contaminants in sediments in the Tamar Estuary, Tasmania, using 210Pb dating and stable Pb isotope analyses. **Environmental Chemistry** 1, 49-54.

Sienkiewicz, E., Gąsiorowski, M., 2016. The evolution of a mining lake-From acidity to natural neutralization. Science of the Total Environment 557-558, 343-354.

Simpson, G.L., Anderson, N.J., 2009. Deciphering the effect of climate change and separating the influence of confounding factors in sediment core records using additive models. Limnology and Oceanography 54, 2529-2541.

Smol, J.P., Stoermer, E.F., 2010. The Diatoms: Applications for the Environmental and Earth Sciences, Second ed. Cambridge University Press, United Kingdom.

Sóskuthy, M., 2017. Generalised additive mixed models for dynamic analysis in linguistics: a practical introduction. arXiv 1703.05339.

Stoddard, J.L., Jeffries, D.S., Lükewille, A., Clair, T.A., Dillon, P.J., Driscoll, C.T., Forsius, M., Johannessen, M., Kahl, J.S., Kellogg, J.H., Kemp, A., Mannio, J., Monteith, D.T., Murdoch, P.S., Patrick, S., Rebsdorf, A., Skjelkvale, B.L.S., M. P., Traaen, T., van Dam, H., Webster, K.E., Wieting, J., Wilander, A., 1999. Regional trends in aquatic recovery from acidification in North America and Europe. Nature 401, 575-578.

Strynadka, N.C., James, M.N., 1989. Crystal structures of the helix-loop-helix calcium-binding proteins. Annual review of biochemistry 58, 951-999.

Teasdale, P.R., Apte, S.C., Ford, P.W., Batley, G.E., Koehnken, L., 2003. Geochemical cycling and speciation of copper in waters and sediments of Macquarie Harbour, Western Tasmania. Estuarine, Coastal and Shelf Science 57, 475-487.

Telford, K., Maher, W., Krikowa, F., Foster, S., 2008. Measurement of total antimony and antimony species in mine contaminated soils by ICPMS and HPLC-ICPMS. Journal of Environmental Monitoring 10, 136.

Tyler, P.A., 1974. Limnological Studies, in: Williams, W.D. (Ed.), Biogeography and Ecology in Tasmania. Dr. W. Junk b.v., Publishers, The Hague, Dordrecht , Netherlands, pp. 29-61.

Tyler, P.A., 1992. A lakeland from the dreamtime the second founders' lecture. British Phycological Journal 27, 353-368.

van Dam, H., Mertens, A., Sinkeldam, J., 1994. A coded checklist and ecological indicator values of freshwater diatoms from The Netherlands. Netherlands Journal of Aquatic Ecology 28, 117-133.

van Dam, H., Suurmond, G., ter Braak, C.J., 1981. Impact of acidification on diatoms and chemistry of Dutch moorland pools. Hydrobiologia 83, 425-459.

Van de Vijver, B., Moravcova, A., Kusber, W.-H., Neustupa, J., 2013. Analysis of the type material of Pinnularia divergentissima (Grunow in Van Heurck) Cleve (Bacillariophyceae). Fottea, Olomouc 13, 1-14.

Vyverman, W., Vyverman, R., Hodgson, D., Tyler, P., 1995. Diatoms from Tasmanian mountain lakes: a reference data-set for environmental reconstruction. The TASDIAT diatom training set: a systematic and autoecological study. Cramer, Berlin.

Vyverman, W., Vyverman, R., Rajendran, V.S., Tyler, P., 1996. Distribution of benthic diatom assemblages in Tasmanian highland lakes and their possible use as indicators of environmental changes. Canadian Journal of Fisheries and Aquatic Sciences 53, 493-508.

Whitlock, C., Larsen, C., 2001. Charcoal as a fire proxy, in: Smol, J.P., Birks, H.J.B., Last, W.M. (Eds.), Tracking Environmental Change Using Lake Sediments. Volume 3: Terrestrial, Algal, and Siliceous Indicators. Kluwer Academic Publishers, Dordrecht, The Netherlands, pp. 75-97.

Winder, M., Schindler, D.E., 2004. Climate change uncouples trophic interactions in an aquatic ecosystem. Ecology 85, 2100-2106.

Wood, S., 2016. Package: mgcv, Mixed GAM Computation Vehicle with GCV/AIC/REML Smoothness Estimation, 1.8-15 ed.

Wood, S.N., 2011. Fast stable restricted maximum likelihood and marginal likelihood estimation of semiparametric generalized linear models. Journal of the Royal Statistical Society: Statistical Methodology Series B 73, 3-36.

Wood, S.W., Hua, Q., Bowman, D.M.J.S., 2011. Fire-patterned vegetation and the development of organic soils in the lowland vegetation mosaics of south-west Tasmania. Australian Journal of Botany 59, 126-136.

Woodward, C.A., Gadd, P.S., 2019. The potential power and pitfalls of using the X-ray fluorescence molybdenum incoherent: Coherent scattering ratio as a proxy for sediment organic content. Quaternary International 514, 30-43.

Woodward, C.A., Slee, A., Gadd, P., Zawadzki, A., Hamze, H., Parmar, A., Zahra, D., 2018. The role of earthquakes and climate in the formation of diamictic sediments in a New Zealand mountain lake. Quaternary International 470, 130-147.

Younger, P.L., Wolkersdorfer, C., 2004. Mining impacts on the fresh water environment: technical and managerial guidelines for catchment scale management. Mine water and the Environment 23, S2-S80.

Ziegler, M., Jilbert, T., Lange, G.J.d., Lourens, L.J., Reichart, G.-J., 2008. Bromine counts from XRF scanning as an estimate of the marine organic carbon content of sediment cores. Geochem Geophys Geosystems 9, 1-6.